

Deepest Cuts for Benders Decomposition

Mojtaba Hosseini^{*1} and John G. Turner^{†1}

¹The Paul Merage School of Business, University of California, Irvine

Abstract

Since its inception, Benders Decomposition (BD) has been successfully applied to a wide range of large-scale mixed-integer (linear) problems. The key element of BD is the derivation of Benders cuts, which are often not unique. In this paper, we introduce a novel unifying Benders cut selection technique based on a geometric interpretation of cut “depth”, produce deepest Benders cuts based on ℓ_p -norms, and study their properties. Specifically, we show that deepest cuts resolve infeasibility through minimal deviation from the incumbent point, are relatively sparse, and may produce optimality cuts even when classical Benders would require a feasibility cut. Leveraging the duality between separation and projection, we develop a Guided Projections Algorithm for producing deepest cuts while exploiting the combinatorial structure or decomposability of problem instances. We then propose a generalization of our Benders separation problem that brings several well-known cut selection strategies under one umbrella. In particular, we provide systematic ways of selecting the normalization coefficients in the Minimal Infeasible Subsystems method by establishing its connection to our method. Finally, in our tests on facility location problems, we show deepest cuts often reduce both runtime and number of Benders iterations, as compared to other cut selection strategies; and relative to classical Benders, use 1/3 the number of cuts and 1/2 the runtime.

Keywords: Benders Decomposition; Acceleration techniques; Cutting planes; Mixed-integer programs

1 Introduction

Since Benders (1962) originally proposed a procedure for solving Mixed-Integer Linear Programming (MILP) problems that temporarily fixes some variables to produce one or more much easier-to-solve subproblems at the expense of additional inference and algorithm iterations, Benders Decomposition (BD) has increasingly attracted the attention of researchers in the last five decades. Of note, BD has proven very effective in tackling several classes of challenging MILP problems through both the classical as well as the generalized and logic-based variants of the BD algorithm.

The inherent capacity of BD for exploiting the structural properties of problems with complicating variables has made it one of the most prominent exact algorithms for solving large-scale optimization problems. Over the years, BD has grown in its ability to solve a wide range of challenging problems including variants of facility location problems (Magnanti and Wong 1981, Fischetti et al. 2016, 2017), supply chain and network design problems (Keyvanshokoo et al. 2016, Alshamsi and Diabat 2018, Fontaine and Minner 2018, Pearce and Forbes 2018), hub location problems (Contreras et al. 2011, 2012, Maheo et al. 2017, Taherkhani et al. 2020), scheduling and routing problems (Mercier 2008, Papadakos 2009, Adulyasak et al. 2015, Bodur and Luedtke 2016, Bayram and Yaman 2017), healthcare operations (Cho et al. 2014, Naderi et al. 2021), machine learning (Rahimi and Gönen 2021), and variants

^{*}mojtaba.hosseini@uci.edu

[†]john.turner@uci.edu

of stochastic programming problems (Santoso et al. 2005, Adulyasak et al. 2015, Bodur et al. 2016, Rahmaniani et al. 2018, Khassiba et al. 2020, Taherkhani et al. 2021) among several other applications.

BD, at its core, is a relax and “learn from mistakes” procedure (Hooker and Ottosson 2003). In classical BD, this learning mechanism is naturally manifested through Linear Programming (LP) duality and mistakes are “corrected” via Benders feasibility and optimality cuts. These cuts are obtained by solving the dual of the subproblem induced by fixing the complicating variables. The learning mechanism, however, need not be restricted to cuts based on LP duality. Geoffrion (1972) laid the foundation for extending BD to general nonlinear optimization problems, Hooker and Ottosson (2003) introduced logic-based BD for tackling problems with logical constraints, and Codato and Fischetti (2006) tailored this idea to MILP problems involving big-M constraints. By treating the separation problem as a feasibility problem, we establish a duality between separation and projection, which we use for deriving what we call *deepest Benders cuts*. With this perspective, the learning component in our Benders procedure can be viewed as resolving infeasibility in this feasibility problem through minimal deviation from the incumbent point.

Despite its promising structure, a naïve implementation of BD may suffer from slow convergence and other computational deficiencies. A wealth of studies have addressed different drawbacks of BD from different angles (see e.g., Rahmaniani et al. 2017, and references therein for recent advancements). As with any other cutting-plane algorithm, the convergence rate is directly tied to the effectiveness of the generated cuts. Given that there is typically more than one way to generate a Benders cut, an important theoretical and practical question is how to select the most “effective” cut(s) in each iteration, with the aim of speeding up convergence. This question has spawned a stream of research, which we contribute to.

In their seminal paper, Magnanti and Wong (1981) introduced a general-purpose cut selection strategy for selecting a nondominated (or Pareto-optimal) optimality cut among the alternative optimal solutions of the subproblem. More recently, Fischetti et al. (2010) cast the Benders subproblem as a feasibility problem, and proposed an alternative cut selection criterion that approximately identifies a minimal source of infeasibility from the derived feasibility problem. Saharidis and Ierapetritou (2010) introduced the Maximum Feasibility Subsystem (MFS) cut generation strategy for accelerating BD in problems where the majority of cuts generated are feasibility (as opposed to optimality) cuts. Sherali and Lunday (2013) treated cut generation as a multi-objective optimization problem and proposed generating maximal nondominated cuts which they showed can be produced by perturbing the right-hand-side of the primal subproblem. Recently, Bodur and Luedtke (2016) and Bodur et al. (2016) proposed methods for sharpening Benders cuts using mixed-integer rounding schemes.

We depart from these studies by (i) taking the “depth” of the candidate cuts explicitly into account, (ii) providing a unifying framework for producing deep optimality and feasibility cuts, and (iii) introducing Benders distance functions that bring several cut selection strategies under one umbrella. We begin Section 1.1 with an outline of the classical BD algorithm, which we then contrast to our alternative decomposition scheme in Section 1.2. This paves the way for us to formally define what we mean by “deep” Benders cuts. In Section 2, we introduce a procedure to produce a so-called “deepest Benders cut” by taking the Euclidean depth of the candidate cuts as a measure of cut quality. Then we extend the notion of depth using general ℓ_p -norms in Section 2.2 and provide a comprehensive study of the properties of deepest cuts in Section 2.3. In Section 3, we introduce Benders distance functions and establish an important monotonicity property tied to convexity that generalizes geometric distance. In Section 4, we (i) present some useful reformulations of the separation problem we use to generate deep cuts, (ii) introduce distance functions based on linear normalization functions, and (iii) present several ways of deriving effective normalization coefficients for our linear normalization functions, which connect our method to other cut selection strategies by Fischetti et al. (2010), Magnanti and Wong (1981) and Conforti and Wolsey (2019). Next, we introduce our Guided Projections Algorithm (GPA)

in Section 5, which leverages combinatorial structure to further accelerate deep cut generation. Then, in Section 6, we run computational experiments on the capacitated facility location problem to test the performance of Bender’s cuts generated using several families of distance functions and demonstrate that deepest cuts produced using GPA require 1/3 the number of cuts and 1/2 the runtime of classical Benders cuts. Finally, we summarize our conclusions in Section 7.

1.1 Classical Benders Decomposition

We begin with a brief outline of the classical Benders Decomposition (BD) algorithm. Consider the MILP problem

$$\begin{aligned} \text{[OP]} \quad \min \quad & \mathbf{c}^\top \mathbf{x} + \mathbf{f}^\top \mathbf{y} \\ \text{s.t.} \quad & A\mathbf{x} + B\mathbf{y} \geq \mathbf{b} \\ & \mathbf{x} \geq \mathbf{0}, \mathbf{y} \in Y, \end{aligned} \tag{1}$$

where $\mathbf{f} \in \mathbb{R}^n$, $\mathbf{c} \in \mathbb{R}^n$, $\mathbf{b} \in \mathbb{R}^m$, matrices A and B are conformable, and $Y \subset \mathbb{Z}^n$ is the domain of the \mathbf{y} -variables. In what follows, we reserve i and j for indexing the rows and columns of B , respectively. For the sake of generality, we do not make any specific assumptions about the structure of the problem, except that it is a general bounded MILP.

The idea behind BD is to project the original problem (OP) from the space of the (\mathbf{x}, \mathbf{y}) -variables onto the space of the \mathbf{y} -variables in the form of

$$\min \{Q(\mathbf{y}) : \mathbf{y} \in Y \cap \text{dom}(Q)\}, \tag{2}$$

where $Q(\mathbf{y}) = \mathbf{f}^\top \mathbf{y} + \tilde{Q}(\mathbf{y})$ and $\tilde{Q}(\mathbf{y})$ accounts for the contribution of the \mathbf{x} -variables to the objective function and is defined as

$$\text{[PSP]} \quad \tilde{Q}(\mathbf{y}) = \min \{ \mathbf{c}^\top \mathbf{x} : A\mathbf{x} \geq \mathbf{b} - B\mathbf{y}, \mathbf{x} \geq \mathbf{0} \}. \tag{3}$$

Problem (3) is known as the primal subproblem (PSP) and $\text{dom}(Q)$ is the set of \mathbf{y} values that induce a feasible PSP. Since OP is bounded, PSP is also bounded for any $\mathbf{y} \in Y$. The classical BD algorithm works as follows. First, problem (2) is reformulated in epigraph form as

$$\min \{ \eta : (\mathbf{y}, \eta) \in \mathcal{E}, \mathbf{y} \in Y \}, \tag{4}$$

where \mathcal{E} is the epigraph of Q defined as

$$\mathcal{E} = \{ (\mathbf{y}, \eta) \in \mathbb{R}^{n+1} : \eta \geq Q(\mathbf{y}), \mathbf{y} \in \text{dom}(Q) \}.$$

Then, a relaxation of (4) is successively tightened by progressively outer-approximating \mathcal{E} with supporting hyperplanes obtained by evaluating, at given \mathbf{y} values, the dual of (3) formulated as

$$\text{[DSP]} \quad \tilde{Q}(\mathbf{y}) = \max \{ \mathbf{u}^\top (\mathbf{b} - B\mathbf{y}) : \mathbf{u}^\top A \leq \mathbf{c}^\top, \mathbf{u} \geq \mathbf{0} \}, \tag{5}$$

which is known as the dual subproblem (DSP). From this dual formulation, we can observe that $\tilde{Q}(\mathbf{y})$ is a piece-wise linear convex function of \mathbf{y} . Thus, $Q(\mathbf{y}) = \mathbf{f}^\top \mathbf{y} + \tilde{Q}(\mathbf{y})$ is a piece-wise linear convex function and \mathcal{E} is a closed convex set. Let \mathcal{U} denote the polyhedron defining the set of feasible solutions of DSP, with \mathcal{U}^* its set of extreme points. For $\mathbf{y} \in \text{dom}(Q)$, the DSP induced by \mathbf{y} is bounded and its optimal value is attained at one of the extreme points of \mathcal{U} . Additionally, since $\tilde{Q}(\mathbf{y})$ is the optimal value of DSP, it follows from weak duality that

$$Q(\mathbf{y}) = \mathbf{f}^\top \mathbf{y} + \tilde{Q}(\mathbf{y}) \geq \mathbf{f}^\top \mathbf{y} + \hat{\mathbf{u}}^\top (\mathbf{b} - B\mathbf{y}) \quad \forall \hat{\mathbf{u}} \in \mathcal{U}.$$

On the other hand, by Farkas lemma, the values of \mathbf{y} that induce an infeasible PSP (i.e., an unbounded DSP) are the ones for which $\hat{\mathbf{v}}^\top(\mathbf{b} - B\mathbf{y}) > 0$ for some (extreme) ray $\hat{\mathbf{v}}$ of \mathcal{U} . Hence, $\text{dom}(Q)$ may be defined as $\text{dom}(Q) = \{\mathbf{y} : 0 \geq \hat{\mathbf{v}}^\top(\mathbf{b} - B\mathbf{y}) \ \forall \hat{\mathbf{v}} \in \mathcal{V}^*\}$, where \mathcal{V}^* is the set of extreme rays of \mathcal{U} . Putting these pieces together, we can rewrite (4) as

$$[\text{CMP}] \min \quad \eta \tag{6}$$

$$\text{s.t.} \quad \eta \geq \mathbf{f}^\top \mathbf{y} + \hat{\mathbf{u}}^\top (\mathbf{b} - B\mathbf{y}) \quad \forall \hat{\mathbf{u}} \in \mathcal{U}^* \tag{7}$$

$$0 \geq \hat{\mathbf{v}}^\top (\mathbf{b} - B\mathbf{y}) \quad \forall \hat{\mathbf{v}} \in \mathcal{V}^* \tag{8}$$

$$\eta \in \mathbb{R}, \mathbf{y} \in Y, \tag{9}$$

which we refer to as the classical Benders master problem (CMP). Constraint sets (7) and (8) are known as the *Benders optimality* and *feasibility* cuts, respectively. The classical BD algorithm solves CMP by initially relaxing these constraints, and at each iteration posts one or more cuts of the form (7) or (8) to this relaxation of CMP until the optimality gap is sufficiently closed. For a complete description of the BD algorithm the reader is referred to Rahmaniani et al. (2017).

1.2 A Unifying Decomposition Scheme

In classical BD, \mathbf{y} is the only piece of information passed from the master problem to the subproblems, and η is merely used to obtain a lower bound on OP. But ignoring η is a little like generating cuts with one hand tied behind your back; you can do it if you have to, but you'll get better results if you don't. We instead begin by reformulating the original problem (1) in epigraph form as

$$\begin{aligned} \min \quad & \eta \\ \text{s.t.} \quad & \eta \geq \mathbf{c}^\top \mathbf{x} + \mathbf{f}^\top \mathbf{y} \\ & A\mathbf{x} + B\mathbf{y} \geq \mathbf{b} \\ & \mathbf{x} \geq \mathbf{0}, \mathbf{y} \in Y, \end{aligned} \tag{10}$$

and apply BD to it by taking (\mathbf{y}, η) as the master problem variables. While this reformulation is sometimes prone to numerical instabilities in the primal space (Bonami et al. 2020), if treated carefully, it provides a framework for unifying the classical Benders optimality and feasibility cuts (Fischetti et al. 2010). Taking this viewpoint, the primal subproblem induced by trial solution $(\hat{\mathbf{y}}, \hat{\eta})$ is

$$\begin{aligned} [\text{FSP}] \min \quad & 0 \\ \text{s.t.} \quad & -\mathbf{c}^\top \mathbf{x} \geq \mathbf{f}^\top \hat{\mathbf{y}} - \hat{\eta} \\ & A\mathbf{x} \geq \mathbf{b} - B\hat{\mathbf{y}} \\ & \mathbf{x} \geq \mathbf{0}, \end{aligned} \tag{11}$$

which is a feasibility problem for any given $(\hat{\mathbf{y}}, \hat{\eta})$, hence we call it the *feasibility subproblem* (FSP). Assigning the dual variable π_0 to the first constraint and the dual vector $\boldsymbol{\pi}$ to the second set of constraints, a Farkas certificate for infeasibility of FSP can be produced using

$$[\text{CGSP}] \max_{(\boldsymbol{\pi}, \pi_0) \in \Pi} \quad \boldsymbol{\pi}^\top (\mathbf{b} - B\hat{\mathbf{y}}) + \pi_0 (\mathbf{f}^\top \hat{\mathbf{y}} - \hat{\eta}), \tag{12}$$

which we refer to as the *certificate generating subproblem* (CGSP), where

$$\Pi = \{(\boldsymbol{\pi}, \pi_0) : \boldsymbol{\pi}^\top A \leq \pi_0 \mathbf{c}^\top, \boldsymbol{\pi} \geq \mathbf{0}, \pi_0 \geq 0\}$$

is the cone of feasible solutions (rays). If FSP is feasible, then the optimal value of both FSP and CGSP is zero. Otherwise, CGSP is unbounded and a ray $(\hat{\boldsymbol{\pi}}, \hat{\pi}_0)$ exists such that $\hat{\boldsymbol{\pi}}^\top (\mathbf{b} - B\hat{\mathbf{y}}) + \hat{\pi}_0 (\mathbf{f}^\top \hat{\mathbf{y}} - \hat{\eta}) > 0$; hence, the infeasible solution $(\hat{\mathbf{y}}, \hat{\eta})$ violates the constraint

$$\hat{\boldsymbol{\pi}}^\top (\mathbf{b} - B\mathbf{y}) + \hat{\pi}_0 (\mathbf{f}^\top \mathbf{y} - \eta) \leq 0.$$

Given $(\hat{\boldsymbol{\pi}}, \hat{\pi}_0) \in \Pi$, we define $\mathcal{H}(\hat{\boldsymbol{\pi}}, \hat{\pi}_0)$ and $\partial(\hat{\boldsymbol{\pi}}, \hat{\pi}_0)$ as the half-space and hyperplane defined by $(\hat{\boldsymbol{\pi}}, \hat{\pi}_0)$, respectively, i.e.,

$$\begin{aligned}\mathcal{H}(\hat{\boldsymbol{\pi}}, \hat{\pi}_0) &= \{(\mathbf{y}, \eta) : \hat{\boldsymbol{\pi}}^\top (\mathbf{b} - B\mathbf{y}) + \hat{\pi}_0(\mathbf{f}^\top \mathbf{y} - \eta) \leq 0\}, \\ \partial(\hat{\boldsymbol{\pi}}, \hat{\pi}_0) &= \{(\mathbf{y}, \eta) : \hat{\boldsymbol{\pi}}^\top (\mathbf{b} - B\mathbf{y}) + \hat{\pi}_0(\mathbf{f}^\top \mathbf{y} - \eta) = 0\}.\end{aligned}$$

Consequently, OP can be restated as the following modified master problem (MP):

$$[\text{MP}] \min \quad \eta \tag{13}$$

$$\text{s.t.} \quad (\mathbf{y}, \eta) \in \mathcal{H}(\hat{\boldsymbol{\pi}}, \hat{\pi}_0) \quad \forall (\hat{\boldsymbol{\pi}}, \hat{\pi}_0) \in \Pi \tag{14}$$

$$\eta \in \mathbb{R}, \mathbf{y} \in Y. \tag{15}$$

More precisely, this is a projection of (10) onto the (\mathbf{y}, η) space. With this representation of BD, at iteration t , we produce a candidate point $(\mathbf{y}^{(t)}, \eta^{(t)})$ by solving a relaxation of MP, and test its feasibility using CGSP. If the test proves $(\mathbf{y}^{(t)}, \eta^{(t)})$ infeasible, we generate a certificate $(\hat{\boldsymbol{\pi}}, \hat{\pi}_0)$ and add a cut of the form (14) to the relaxed MP to avoid producing the infeasible $(\mathbf{y}^{(t)}, \eta^{(t)})$ again; otherwise, we conclude that $(\mathbf{y}^{(t)}, \eta^{(t)})$ is an optimal solution for MP. As noted in Proposition 1 below, cuts of the form (14) represent both Benders optimality and feasibility cuts; when $\hat{\pi}_0 > 0$, the cut corresponds to a classical Benders optimality cut, while $\hat{\pi}_0 = 0$ corresponds to a classical Benders feasibility cut. An overview of the BD algorithm based on this decomposition scheme is presented in Algorithm 1. We have omitted proofs from the body of this manuscript, but proofs for all of our theorems and propositions can be found in Appendix A.

Proposition 1. *Solution (\mathbf{y}, η) satisfies constraints (14) if and only if $(\mathbf{y}, \eta) \in \mathcal{E}$.*

Algorithm 1 Overview of Benders Decomposition algorithm

- 1: $t \leftarrow 1, \hat{\Pi}_t \leftarrow \emptyset$.
 - 2: Solve MP with $\hat{\Pi}_t$ in place of Π and obtain master solution $(\mathbf{y}^{(t)}, \eta^{(t)})$.
 - 3: Find a certificate $(\hat{\boldsymbol{\pi}}, \hat{\pi}_0)$ for infeasibility of $(\mathbf{y}^{(t)}, \eta^{(t)})$ using CGSP (12).
 - 4: **if** certificate $(\hat{\boldsymbol{\pi}}, \hat{\pi}_0)$ exists **then**
 - 5: Set $\hat{\Pi}_{t+1} \leftarrow \hat{\Pi}_t \cup \{(\hat{\boldsymbol{\pi}}, \hat{\pi}_0)\}$, $t \leftarrow t + 1$ and go to step 2.
 - 6: **else**
 - 7: Stop. $(\mathbf{y}^{(t)}, \eta^{(t)})$ is an optimal solution for MP.
 - 8: **end if**
-

At step 3 of Algorithm 1, CGSP provides a logical answer to whether the current master problem solution $(\mathbf{y}^{(t)}, \eta^{(t)})$ is feasible (and hence optimal) for MP. But, not every logical answer is equally useful. In other words, to prove suboptimality of $(\mathbf{y}^{(t)}, \eta^{(t)})$, CGSP produces a certificate $(\hat{\boldsymbol{\pi}}, \hat{\pi}_0) \in \Pi$ such that $\hat{\boldsymbol{\pi}}^\top (\mathbf{b} - B\mathbf{y}^{(t)}) + \hat{\pi}_0(\mathbf{f}^\top \mathbf{y}^{(t)} - \eta^{(t)}) > 0$, without providing further information about how “far” $(\mathbf{y}^{(t)}, \eta^{(t)})$ is from being optimal. Moreover, not only do we want to discard the trial solution $(\mathbf{y}^{(t)}, \eta^{(t)})$, but we also want to rule out as many other unacceptable values of (\mathbf{y}, η) as possible. Hence, we may phrase the key question of the BD algorithm as: *How should we select a certificate $(\hat{\boldsymbol{\pi}}, \hat{\pi}_0) \in \Pi$ that conveys additional information about the suboptimality of $(\mathbf{y}^{(t)}, \eta^{(t)})$, so that we may exploit this information to speed up the convergence of the BD algorithm?* Our order of business in this article is to address this question by introducing selection strategies that exploit the properties of promising cuts in a computationally tractable manner.

2 Deepest Benders Cuts

At each iteration of the BD Algorithm 1, we wish to separate (if possible) the incumbent point $(\mathbf{y}^{(t)}, \eta^{(t)})$ from the epigraph \mathcal{E} . As a result of Proposition 1, we may equivalently define \mathcal{E} as

$$\mathcal{E} = \{(\mathbf{y}, \eta) : (\mathbf{y}, \eta) \in \mathcal{H}(\hat{\boldsymbol{\pi}}, \hat{\pi}_0) \quad \forall (\hat{\boldsymbol{\pi}}, \hat{\pi}_0) \in \Pi\}.$$

In cutting-plane theory, the separation problem produces a hyperplane (or a cut) that lies between a given point and a closed convex set. In our application, we want to separate the incumbent point $(\mathbf{y}^{(t)}, \eta^{(t)})$ from the closed convex set \mathcal{E} using a hyperplane $\partial(\boldsymbol{\pi}, \pi_0)$ for some $(\boldsymbol{\pi}, \pi_0) \in \Pi$. Note that infinitely many such hyperplanes may exist, thus one needs a selection criterion for producing the cut that “best” separates $(\mathbf{y}^{(t)}, \eta^{(t)})$ from \mathcal{E} . While there is no universal definition of “best” cut, a “good” cut should satisfy some natural requirements. First, it should be a supporting hyperplane for \mathcal{E} , in the sense that it should touch \mathcal{E} at some point. We further postulate that the cut must be *deep*, in the sense that it is as far from the given point $(\mathbf{y}^{(t)}, \eta^{(t)})$ as possible. We begin in Section 2.1 with the Euclidean distance as our measure of cut depth, then generalize to distances induced by ℓ_p -norms in Section 2.2. Finally, in Section 2.3 we present an alternative primal perspective of deepest cut generation, and derive some important properties of deepest cuts. Specifically, we show that deepest cuts not only support \mathcal{E} , but also (i) minimally resolve infeasibility in the system FSP, (ii) amount to optimality cuts, and (iii) are relatively flat thus, help close the gap quickly.

2.1 Euclidean Deepest Cuts

As our measure of cut depth, we start with the Euclidean distance from the point $(\hat{\mathbf{y}}, \hat{\eta})$ to the hyperplane $\partial(\boldsymbol{\pi}, \pi_0)$. Euclidean norm is the standard norm used in convex analysis, and measuring depth using this norm, also known as scaled violation, is also common practice in cutting-plane theory. For example, to produce deep facet-defining cuts for solving mixed-integer programs, Balas et al. (1993) and Cadoux (2010) use the Euclidean distance between the optimal vertex of the current relaxation and candidate separating hyperplanes; in a similar spirit, we also call the cuts we generate *deepest Benders cuts*.

Let $d(\hat{\mathbf{y}}, \hat{\eta} | \boldsymbol{\pi}, \pi_0)$ be the Euclidean distance between the point $(\hat{\mathbf{y}}, \hat{\eta})$ and the hyperplane $\partial(\boldsymbol{\pi}, \pi_0)$. From basic linear algebra, we know that the Euclidean distance from the point $\hat{\mathbf{z}}$ to the hyperplane $\boldsymbol{\alpha}^\top \mathbf{z} + \beta = 0$ is $\frac{|\boldsymbol{\alpha}^\top \hat{\mathbf{z}} + \beta|}{\|\boldsymbol{\alpha}\|_2}$. Hence,

$$d(\hat{\mathbf{y}}, \hat{\eta} | \boldsymbol{\pi}, \pi_0) = \frac{|\boldsymbol{\pi}^\top (\mathbf{b} - B\hat{\mathbf{y}}) + \pi_0(\mathbf{f}^\top \hat{\mathbf{y}} - \hat{\eta})|}{\|(\pi_0 \mathbf{f}^\top - \boldsymbol{\pi}^\top B, \pi_0)\|_2} = \frac{\boldsymbol{\pi}^\top (\mathbf{b} - B\hat{\mathbf{y}}) + \pi_0(\mathbf{f}^\top \hat{\mathbf{y}} - \hat{\eta})}{\|(\pi_0 \mathbf{f}^\top - \boldsymbol{\pi}^\top B, \pi_0)\|_2}, \quad (16)$$

where the last equality holds because $(\hat{\mathbf{y}}, \hat{\eta})$ must (except at the last Benders iteration) violate the constraint $\boldsymbol{\pi}^\top (\mathbf{b} - B\mathbf{y}) + \pi_0(\mathbf{f}^\top \mathbf{y} - \eta) \leq 0$, hence $\boldsymbol{\pi}^\top (\mathbf{b} - B\hat{\mathbf{y}}) + \pi_0(\mathbf{f}^\top \hat{\mathbf{y}} - \hat{\eta}) \geq 0$. To produce a deepest cut, we choose $(\boldsymbol{\pi}, \pi_0) \in \Pi$ which maximizes this distance (i.e., depth) via

$$[\text{SSP}] \quad d^*(\hat{\mathbf{y}}, \hat{\eta}) = \max_{(\boldsymbol{\pi}, \pi_0) \in \Pi} d(\hat{\mathbf{y}}, \hat{\eta} | \boldsymbol{\pi}, \pi_0),$$

which we refer to as the *separation subproblem (SSP)*. As we will show in Section 2.3, maximizing the distance of a separating hyperplane from the point $(\hat{\mathbf{y}}, \hat{\eta})$ coincides with finding the minimum distance of $(\hat{\mathbf{y}}, \hat{\eta})$ from the epigraph \mathcal{E} ; thus we call $d^*(\hat{\mathbf{y}}, \hat{\eta})$ the (Euclidean) distance of $(\hat{\mathbf{y}}, \hat{\eta})$ from the epigraph \mathcal{E} . At iteration t of the BD algorithm, if $d^*(\mathbf{y}^{(t)}, \eta^{(t)}) > 0$, then we can separate $(\mathbf{y}^{(t)}, \eta^{(t)})$ from \mathcal{E} , otherwise $(\mathbf{y}^{(t)}, \eta^{(t)}) \in \mathcal{E}$. Consequently, if $d^*(\mathbf{y}^{(t)}, \eta^{(t)}) = 0$, then $(\mathbf{y}^{(t)}, \eta^{(t)})$ is an optimal solution for MP.

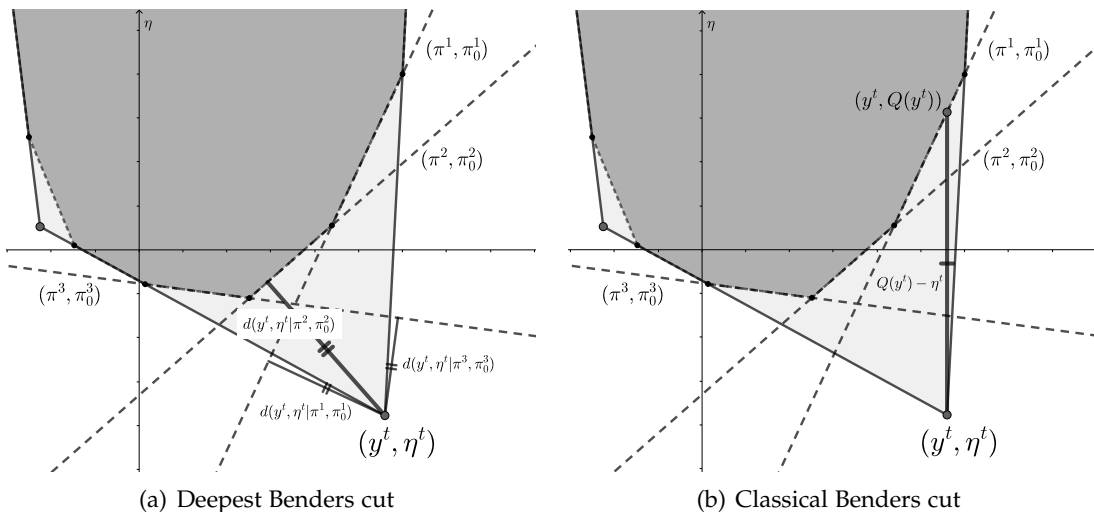


Figure 1: Deepest (a) versus classical (b) Benders cut selection. The dark and light polygons represent \mathcal{E} and the approximation of \mathcal{E} at iteration t (i.e., \mathcal{E}_t), respectively. (\mathbf{y}^t, η^t) is the current solution of the master problem to be separated. The dashed lines represent the hyperplanes associated with the dual solutions. The dual solution selected by the classical Benders subproblem is (π^1, π_0^1) whereas the solution selected based on Euclidean distance is (π^2, π_0^2) .

Figure 1(a) illustrates how we select a certificate (π, π_0) by finding the hyperplane that is the maximum Euclidean distance from the master problem's solution (\mathbf{y}^t, η^t) . For demonstration purposes, we assume y is a continuous one-dimensional variable in this toy example. As illustrated in Figure 1(b), the hyperplane produced by classical DSP supports \mathcal{E} at $(\mathbf{y}^t, Q(\mathbf{y}^t))$. While the deepest cuts also support \mathcal{E} (see Proposition 3), it does not necessarily do so at $(\mathbf{y}^t, Q(\mathbf{y}^t))$, but at a point which we call the *projection of (\mathbf{y}^t, η^t) onto \mathcal{E}* . As illustrated in Figure 1(a), dual solutions (π^1, π_0^1) , (π^2, π_0^2) and (π^3, π_0^3) (and their convex combinations) are the candidate solutions evaluated based on the Euclidean distance of their associated hyperplanes to the point (\mathbf{y}^t, η^t) , and (π^2, π_0^2) is selected as the deepest cut. It is worth pointing out that in the literature, the question of which Benders cut to select usually arises when the classical DSP admits alternative optimal solutions (Magnanti and Wong 1981). However, even when the classical DSP admits a unique optimal solution (as in the given example), the deepest cut may not coincide with the classical Benders cut.

2.2 ℓ_p -norm deepest Cuts

We now generalize our notion of distance to that induced by any ℓ_p -norm. Our derivation begins with the observation that the denominator in (16) is the ℓ_2 -norm of the vector of coefficients $(\pi_0 \mathbf{f}^\top - \pi^\top B, \pi_0)$. If we replace this norm with a general ℓ_p -norm for $p \geq 1$, and define d_{ℓ_p} as

$$d_{\ell_p}(\hat{\mathbf{y}}, \hat{\eta} | \pi, \pi_0) = \frac{\pi^\top (\mathbf{b} - B\hat{\mathbf{y}}) + \pi_0 (\mathbf{f}^\top \hat{\mathbf{y}} - \hat{\eta})}{\|(\pi_0 \mathbf{f}^\top - \pi^\top B, \pi_0)\|_p}, \quad (17)$$

then an ℓ_p -norm deepest cut (or ℓ_p -deepest cut for short) can be produced by solving the following separation problem

$$[\text{SSP}] d_{\ell_p}^*(\hat{\mathbf{y}}, \hat{\eta}) = \max_{(\pi, \pi_0) \in \Pi} d_{\ell_p}(\hat{\mathbf{y}}, \hat{\eta} | \pi, \pi_0). \quad (18)$$

With this definition, d_{ℓ_p} still measures the distance of $(\hat{\mathbf{y}}, \hat{\eta})$ from the hyperplane $\partial(\pi, \pi_0)$, but unlike for the special case where $p = 2$ (Euclidean distance), the distance measure is no longer the ℓ_p -distance.

In fact, as Proposition 2 shows below, d_{ℓ_p} measures the distance between $(\hat{\mathbf{y}}, \hat{\eta})$ and the hyperplane $\partial(\boldsymbol{\pi}, \pi_0)$ with respect to the dual norm ℓ_q , where $\frac{1}{p} + \frac{1}{q} = 1$. The proof of this result relies on the definition of dual norm and is proven for general norms (including standard ℓ_p norms), but to be expositionally consistent we state the results for standard ℓ_p norms.

Proposition 2. *Given $q \geq 1$ and $\hat{\mathbf{z}} \in \mathbb{R}^{n+1}$, the minimum ℓ_q -distance from the point $\hat{\mathbf{z}}$ to the points on the hyperplane $\boldsymbol{\alpha}^\top \mathbf{z} + \beta = 0$ is*

$$\min_{\mathbf{z}: \boldsymbol{\alpha}^\top \mathbf{z} + \beta = 0} \|\mathbf{z} - \hat{\mathbf{z}}\|_q = \frac{|\boldsymbol{\alpha}^\top \hat{\mathbf{z}} + \beta|}{\|\boldsymbol{\alpha}\|_p},$$

where ℓ_p is the dual norm of ℓ_q (i.e., $\frac{1}{p} + \frac{1}{q} = 1$).

Note that, as given in the proof of Proposition 2, we may extend the definition of deepest cuts by replacing the denominator in (17) with general norms (e.g., a composition of ℓ_p -norms with different p for different subsets of the components of $(\pi_0 \mathbf{f}^\top - \boldsymbol{\pi}^\top B, \pi_0)$). However, for clarity and simplicity of exposition, we restrict consideration in the remainder of this paper to standard ℓ_p -norms.

Some choices of p for ℓ_p -deepest cuts merit special attention. In particular, for $p = 1$ and $p = \infty$, d_{ℓ_p} defined by (17) measures the ℓ_∞ and ℓ_1 distance of $(\hat{\mathbf{y}}, \hat{\eta})$ from the hyperplane $\partial(\boldsymbol{\pi}, \pi_0)$, respectively. As we will show in Section 4.1, these norms are in general computationally favorable over the ℓ_2 -norm since they result in linear separation subproblems.

As well, note that π_0 is the coefficient of η and $\boldsymbol{\pi}^\top B - \pi_0 \mathbf{f}^\top$ is the coefficient of \mathbf{y} in the cut $\boldsymbol{\pi}^\top \mathbf{b} \leq (\boldsymbol{\pi}^\top B - \pi_0 \mathbf{f}^\top) \mathbf{y} + \pi_0 \eta$. Therefore, deepest cuts effectively cut off the point $(\hat{\mathbf{y}}, \hat{\eta})$ while minimizing the coefficients of the variables in the produced constraint. In particular, when the ℓ_1 -norm is employed, producing deepest cuts mimics the idea of producing maximally nondominated Benders cuts introduced by Sherali and Lunday (2013), where the cut is maximally nondominated in the sense typically used in the cutting-plane theory for integer programs.

2.3 A Primal Projection Perspective of the Separation Problem

We now provide another view of deepest cuts, which will be important for analyzing their properties and paves the way for devising algorithms to produce them efficiently. By strong duality, we establish a duality between separation and projection as stated in Theorem 1 below.

Theorem 1. *Separation problem (18) is equivalent to the following Lagrangian dual problem*

$$\begin{aligned} [\text{Primal SSP}] \quad & \min \quad \|(\mathbf{y} - \hat{\mathbf{y}}, \eta - \hat{\eta})\|_q \\ & \text{s.t.} \quad \eta \geq \mathbf{c}^\top \mathbf{x} + \mathbf{f}^\top \mathbf{y} \\ & \quad \quad \quad A\mathbf{x} \geq \mathbf{b} - B\mathbf{y} \\ & \quad \quad \quad \mathbf{x} \geq \mathbf{0}, \end{aligned} \tag{19}$$

in which $(\mathbf{y}, \mathbf{x}, \eta)$ are the variables and ℓ_q is the dual norm of ℓ_p .

The following result follows from strong duality and the definition of \mathcal{E} .

Corollary 1. *$d_{\ell_p}^*(\hat{\mathbf{y}}, \hat{\eta})$ measures the ℓ_q distance of $(\hat{\mathbf{y}}, \hat{\eta})$ from \mathcal{E} . That is,*

$$d_{\ell_p}^*(\hat{\mathbf{y}}, \hat{\eta}) = \min_{(\mathbf{y}, \eta) \in \mathcal{E}} \|\mathbf{y} - \hat{\mathbf{y}}, \eta - \hat{\eta}\|_q. \tag{20}$$

Let $(\tilde{\mathbf{y}}, \tilde{\eta})$ be the optimal solution of the Primal SSP. In convex analysis, the solution of (20) for $q = 2$ is known as the *projection* of $(\hat{\mathbf{y}}, \hat{\eta})$ onto \mathcal{E} . Thus, we refer to $(\tilde{\mathbf{y}}, \tilde{\eta})$ henceforth as the ℓ_q -projection of

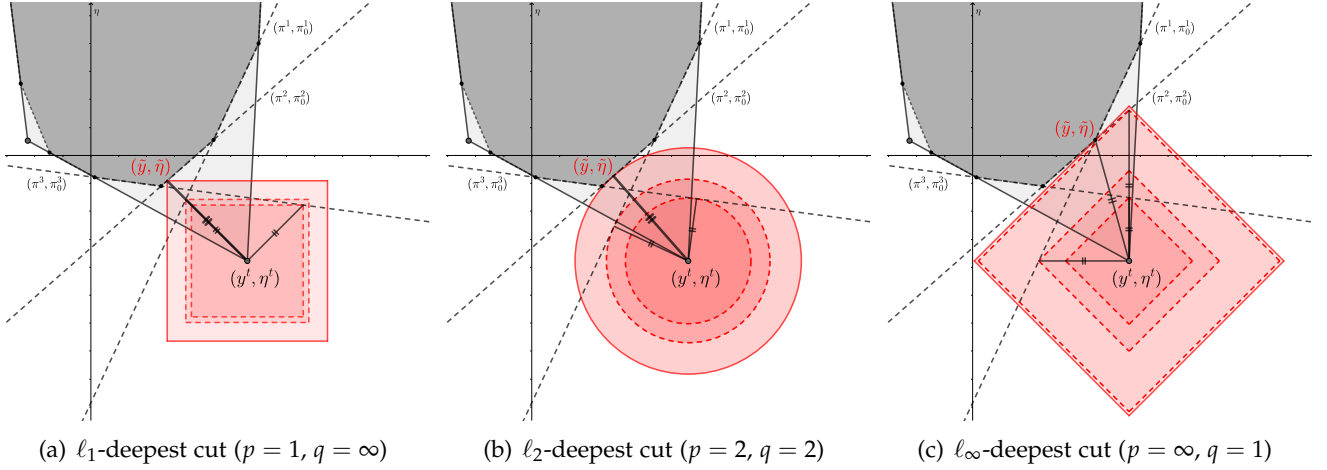


Figure 2: Primal and dual perspectives of the separation problem. The dark and light polygons represent \mathcal{E} and the approximation of \mathcal{E} at iteration t , respectively. The point $(\mathbf{y}^{(t)}, \eta^{(t)})$ is the current solution of the master problem to be separated. Finding the ℓ_p -deepest cut (i.e., normalizing dual solutions with ℓ_p -norm) accounts for resolving infeasibility in FSP (in the primal space) by finding a point in \mathcal{E} with minimum ℓ_q -distance to $(\mathbf{y}^{(t)}, \eta^{(t)})$, where ℓ_q is the dual norm of ℓ_p . The red lines represent the contour lines of the objective value of SSP, which also correspond to ℓ_q -balls around $(\mathbf{y}^{(t)}, \eta^{(t)})$.

$(\hat{\mathbf{y}}, \hat{\eta})$, and refer to (20) as the *projection subproblem*. Figure 2 illustrates these projections for different values of q . Observe that the ℓ_q -projection or the ℓ_p -deepest cut might not be unique for $p = 1$ ($q = \infty$) or $p = \infty$ ($q = 1$). The following proposition states that deepest cuts support \mathcal{E} at ℓ_q -projections, even when the projection or the cut are not unique.

Proposition 3. *Let $(\tilde{\mathbf{y}}, \tilde{\eta}) \in \mathcal{E}$ be an ℓ_q -projection of $(\hat{\mathbf{y}}, \hat{\eta})$ onto \mathcal{E} . Then, any ℓ_p -deepest cut separating $(\hat{\mathbf{y}}, \hat{\eta})$ from \mathcal{E} supports \mathcal{E} at $(\tilde{\mathbf{y}}, \tilde{\eta})$.*

From the duality between separation and projection established in the above Theorem and Proposition, we derive the following important technical results.

Deepest cuts minimally resolve infeasibility in FSP. By Theorem 1 and as illustrated in Figure 2, producing an ℓ_p -deepest cut amounts to finding the point $(\tilde{\mathbf{y}}, \tilde{\eta})$ of least ℓ_q -distance from $(\hat{\mathbf{y}}, \hat{\eta})$ for which a feasible solution \mathbf{x} exists that satisfies the system

$$\left\{ \mathbf{c}^\top \mathbf{x} \leq \tilde{\eta} - \mathbf{f}^\top \tilde{\mathbf{y}}; \quad A\mathbf{x} \geq \mathbf{b} - B\tilde{\mathbf{y}}; \quad \mathbf{x} \geq \mathbf{0} \right\}.$$

Hence, producing a deepest cut can be viewed as resolving infeasibility of FSP (11) through minimal deviation from $(\hat{\mathbf{y}}, \hat{\eta})$ with respect to the ℓ_q -norm. If FSP is feasible for $(\hat{\mathbf{y}}, \hat{\eta})$ (i.e., if $\|\hat{\mathbf{y}} - \hat{\mathbf{y}}, \hat{\eta} - \hat{\eta}\|_q = 0$), then $(\hat{\mathbf{y}}, \hat{\eta})$ is optimal for MP. Effectively, $d_{\ell_p}^*(\hat{\mathbf{y}}, \hat{\eta})$ measures how far $(\hat{\mathbf{y}}, \hat{\eta})$ is from being optimal by measuring the minimal deviation in $(\hat{\mathbf{y}}, \hat{\eta})$ that renders FSP feasible. Thus, producing a deepest cut assesses how inaccurate our guess of the optimal solution is.

Sparsity, density and flatness of deepest cuts. We have empirically observed that the deepest cuts generated at the early stages of the BD algorithm tend to be (relatively) flat. That is, the coefficients of the \mathbf{y} -variables in the cut are mostly zero, and in some cases the cut is completely flat, i.e., all \mathbf{y} coefficients are zero. Here, we provide a justification for this observation and discuss its implications. Along this vein, we first note the following property of ℓ_1 -deepest cuts.

Proposition 4. *For sufficiently small $\hat{\eta}$, the ℓ_1 -deepest cut separating $(\hat{\mathbf{y}}, \hat{\eta})$ from \mathcal{E} is the flat cut $\eta \geq Q^*$, where $Q^* = \min_{\mathbf{y}} Q(\mathbf{y})$ is the optimal value of Q for unrestricted \mathbf{y} .*

Proposition 4 implies that, at early iterations of the BD algorithm, an ℓ_1 -deepest cut can provide a lower bound of at least Q^* . Since Q^* is obtained by relaxing $\mathbf{y} \in Y$, Q^* is at most equal to the optimal value of the LP relaxation of OP. While the quality of this bound is problem-specific, we have observed that the bound is indeed very close to the optimal value of OP when the integrality gap is low (e.g., in facility location problems).

More generally, for small p (i.e., large q) and relatively small $\hat{\eta}$, we may approximate $\|(\mathbf{y} - \hat{\mathbf{y}}, \eta - \hat{\eta})\|_q \approx \eta - \hat{\eta}$. Therefore, in line with Proposition 4, we can expect that the coefficients of the \mathbf{y} -variables in the ℓ_p -deepest cuts (i.e., $\hat{\pi}_0 \mathbf{f}^\top - \hat{\pi}^\top B$) will be close to zero, which means that the deepest cuts are relatively *sparse*. This observation is also in line with using Lasso or ℓ_1 -regularization in machine learning and statistics for producing sparse solutions (see e.g., Tibshirani 1996). By the same token, large values of p (e.g., $p = \infty$) induce *dense* cuts, in that the coefficients of the \mathbf{y} variables are mostly non-zero.

Deepest cuts are more likely to be optimality cuts than feasibility cuts. In our experiments with deepest cuts, we found that they are likely to be optimality cuts, even when classical Benders produces a feasibility cut (i.e., even when $\hat{\mathbf{y}} \notin \text{dom}(Q)$). Intuitively, since at each iteration of BD, $\eta^{(t)}$ is an under-estimator of the convex piece-wise linear function Q and deepest cuts support \mathcal{E} , the coefficient of η in a deepest cut (namely, π_0) is most likely non-zero (i.e., the cut is an optimality cut). More specifically, Propositions 5 and 6 below provide sufficient conditions for when deepest cuts are guaranteed to be optimality cuts.

Proposition 5. *Let $Q^* = \min_{\mathbf{y}} Q(\mathbf{y})$ be the optimal unrestricted value of Q . Provided that $\hat{\eta} < Q^*$ and $p > 1$, the ℓ_p -deepest cut(s) separating $(\hat{\mathbf{y}}, \hat{\eta})$ are optimality cuts for any arbitrary $\hat{\mathbf{y}}$ (i.e., even if $\hat{\mathbf{y}} \notin \text{dom}(Q)$).*

Proposition 6. *Assume the ℓ_q -projection of $(\hat{\mathbf{y}}, \hat{\eta})$ onto \mathcal{E} is unique, and denote it by the point $(\tilde{\mathbf{y}}, \tilde{\eta})$. If $\hat{\eta} < \tilde{\eta}$, then the ℓ_p -deepest cuts separating $(\hat{\mathbf{y}}, \hat{\eta})$ are optimality cuts for any arbitrary $\hat{\mathbf{y}}$ (i.e., even if $\hat{\mathbf{y}} \notin \text{dom}(Q)$).*

Proposition 5 guarantees that deepest cuts are optimality cuts when $\hat{\eta}$ is sufficiently small. Proposition 6 further suggests that, even if $\hat{\eta}$ is not very small, deepest cuts are more likely to be optimality cuts (note that the ℓ_q -projection is always unique for $1 < q < \infty$). This is particularly appealing from a practical standpoint, as the contribution of Benders optimality cuts to closing the gap is usually more pronounced than that of feasibility cuts (see e.g., Saharidis and Ierapetritou 2010, de Sá et al. 2013). This property of deepest cuts is in line with the cut generation strategy proposed by Saharidis and Ierapetritou (2010), where to speed up convergence, they produce an additional optimality cut whenever a feasibility cut is needed.

3 General Benders Distance Functions

In this section, we introduce a general distance function based on duality theory, which we call a *Benders distance function*. Such a distance function (a) identifies whether the incumbent point $(\hat{\mathbf{y}}, \hat{\eta})$ is inside, outside, or on the boundary of the epigraph \mathcal{E} , and (b) if outside, conveys how “far” the incumbent point is from the boundary. Crucially, we do not explicitly define the metric on which a Benders distance function is based; this is by design, and interestingly is not needed. In fact, we show in Section 3.1 that so long as a monotonicity property linked to convexity holds, then a sufficient notion of distance exists. Then, in Section 3.2 we introduce an important special class of Benders distance function, normalized distance functions, which we will use in Section 4 to connect deepest cuts with other types of Benders cuts from the literature. Finally, in Section 3.3 we introduce a distance-based BD algorithm and study its convergence properties.

3.1 Definition

We define a Benders distance function, which is a generalization of the geometric distance functions induced by ℓ_p -norms presented earlier, as follows.

Definition 1 (Benders distance function). Function $d(\hat{\mathbf{y}}, \hat{\eta} | \boldsymbol{\pi}, \pi_0) : \mathbb{R}^{n+1} \times \Pi \rightarrow \mathbb{R}$ is a Benders distance function if (i) it certifies $d(\hat{\mathbf{y}}, \hat{\eta} | \boldsymbol{\pi}, \pi_0) > 0$ iff $(\hat{\mathbf{y}}, \hat{\eta})$ is in the exterior of $\mathcal{H}(\boldsymbol{\pi}, \pi_0)$, $d(\hat{\mathbf{y}}, \hat{\eta} | \boldsymbol{\pi}, \pi_0) = 0$ iff $(\hat{\mathbf{y}}, \hat{\eta})$ is on the boundary of $\mathcal{H}(\boldsymbol{\pi}, \pi_0)$, and $d(\hat{\mathbf{y}}, \hat{\eta} | \boldsymbol{\pi}, \pi_0) < 0$ iff $(\hat{\mathbf{y}}, \hat{\eta})$ is in the interior of $\mathcal{H}(\boldsymbol{\pi}, \pi_0)$, and (ii) $d^*(\hat{\mathbf{y}}, \hat{\eta})$ defined below is **convex**:

$$[\text{BSP}] \quad d^*(\hat{\mathbf{y}}, \hat{\eta}) = \sup_{(\boldsymbol{\pi}, \pi_0) \in \Pi} d(\hat{\mathbf{y}}, \hat{\eta} | \boldsymbol{\pi}, \pi_0). \quad (21)$$

Definition 2 (Epigraph distance function). For a given Benders distance function d , we call d^* as defined in (21) the epigraph distance function induced by d .

Proposition 7. Epigraph distance function d^* certifies $d^*(\hat{\mathbf{y}}, \hat{\eta}) > 0$ iff $(\hat{\mathbf{y}}, \hat{\eta})$ is in the exterior of \mathcal{E} , $d^*(\hat{\mathbf{y}}, \hat{\eta}) = 0$ iff $(\hat{\mathbf{y}}, \hat{\eta})$ is on the boundary of \mathcal{E} , and $d^*(\hat{\mathbf{y}}, \hat{\eta}) < 0$ iff $(\hat{\mathbf{y}}, \hat{\eta})$ is in the interior of \mathcal{E} .

By Proposition 7, d^* maps each point $(\hat{\mathbf{y}}, \hat{\eta}) \in \mathbb{R}^{n+1}$ to a value in the extended real number line (i.e., $\mathbb{R} \cup \{\pm\infty\}$) such that the sign of $d^*(\hat{\mathbf{y}}, \hat{\eta})$ determines if $(\hat{\mathbf{y}}, \hat{\eta})$ is in the exterior (sign = +1), interior (sign = -1) or on the boundary of \mathcal{E} (sign = 0). The convexity requirement for d^* is tied to the epigraph distance function d^* being monotonic in the following sense.

Definition 3 (Monotonicity of epigraph distance function). For arbitrary $(\hat{\mathbf{y}}, \hat{\eta}) \notin \mathcal{E}$ and $(\mathbf{y}^0, \eta^0) \in \partial\mathcal{E}$ (boundary of \mathcal{E}) such that the open line segment between $(\hat{\mathbf{y}}, \hat{\eta})$ and (\mathbf{y}^0, η^0) lies in the exterior of \mathcal{E} , define $d^*(\alpha) = d^*((1 - \alpha)(\mathbf{y}^0, \eta^0) + \alpha(\hat{\mathbf{y}}, \hat{\eta}))$. We say the epigraph distance function d^* is **monotonic** if $d^*(\alpha_1) \leq d^*(\alpha_2)$ for any $0 \leq \alpha_1 < \alpha_2 \leq 1$. We say d^* is **strongly monotonic** if $d^*(\alpha_1) < d^*(\alpha_2)$ for any $0 \leq \alpha_1 < \alpha_2 \leq 1$.

Intuitively, and as illustrated in Figure 3(b), (strong) monotonicity of d^* implies that as α increases, we move away from the boundary of \mathcal{E} and distance increases (i.e., d^* becomes larger). Theorem 2 formally establishes that $d^*(\hat{\mathbf{y}}, \hat{\eta})$ can be viewed as how far $(\hat{\mathbf{y}}, \hat{\eta})$ is from the boundary of \mathcal{E} . The proof of this result uses the fact that d^* is a convex function.

Theorem 2. Epigraph distance functions are monotonic.

We end this section by pointing out that our definition of Benders distance functions is sufficiently general to allow us to bring several well-known cut selection strategies under one umbrella, which we will discuss in further detail in Section 4. However, in that section we will show that classical Benders cuts, which we would not consider particularly “deep”, can also be generated using a Benders distance function. In essence, just because a function may be classified as a Benders distance function does not automatically mean that strong, deep cuts will be generated using it. For this reason, we henceforth reserve the term “deepest cuts” to mean cuts that are produced based on geometric distance functions (i.e., d_{ℓ_p}), which correspond to what we believe most people would intuitively consider “deep cuts”. Finally, we remark that the epigraph distance functions induced by d_{ℓ_p} are strongly monotonic, which draws another distinction between these distance functions and general Benders distance functions.

Proposition 8. Epigraph distance function $d_{\ell_p}^*$ (18) is strongly monotonic for any $p \geq 1$.

3.2 Normalized Distance Functions and Normalization Functions

We now introduce an important special class of Benders distance functions, which we call *normalized Benders distance functions*. This is a generalization of the geometric ℓ_p -norm-based Benders distance functions that we introduced in Section 2.2. The distance functions in this class are constructed by

replacing the denominator of the distance function d_{ℓ_p} (17) with a general *normalization function* which is only required to be a positive homogeneous function of the dual variables.

Definition 4 (Normalized distance function). Let $d_g(\hat{\mathbf{y}}, \hat{\boldsymbol{\eta}} | \boldsymbol{\pi}, \pi_0) = \frac{\boldsymbol{\pi}^\top (\mathbf{b} - B\hat{\mathbf{y}}) + \pi_0 (\mathbf{f}^\top \hat{\mathbf{y}} - \hat{\boldsymbol{\eta}})}{g(\boldsymbol{\pi}, \pi_0)}$ where g is a positive homogeneous function (i.e., $g(\alpha\boldsymbol{\pi}, \alpha\pi_0) = \alpha g(\boldsymbol{\pi}, \pi_0)$ for any $\alpha \geq 0$). We call d_g a **normalized distance function**, and refer to g as its **normalization function**.

The normalization function g governs the behavior of the distance function, and quantifies our perception of the quality of the cut it produces. Homogeneity of g is critical. Indeed, with constant (i.e., non-homogeneous) $g(\boldsymbol{\pi}, \pi_0) = 1$, BSP is equivalent to the naïve CGSP (12), for which $d^*(\mathbf{y}^{(t)}, \boldsymbol{\eta}^{(t)}) \in \{0, +\infty\}$. In this case, d^* is simply a characteristic function of \mathcal{E} , which, regardless of the quality of the cut, merely provides a binary answer to whether or not $(\mathbf{y}^{(t)}, \boldsymbol{\eta}^{(t)})$ is the optimal solution, without any further indication of how far $(\mathbf{y}^{(t)}, \boldsymbol{\eta}^{(t)})$ is from being optimal.

For a positive homogeneous function g , let $\Pi_g = \{(\boldsymbol{\pi}, \pi_0) \in \Pi : g(\boldsymbol{\pi}, \pi_0) \leq 1\}$ be the cone Π truncated by the constraint $g(\boldsymbol{\pi}, \pi_0) \leq 1$, and define the normalized separation problem (NSP) as

$$[\text{NSP}] \quad \max_{(\boldsymbol{\pi}, \pi_0) \in \Pi_g} \boldsymbol{\pi}^\top (\mathbf{b} - B\hat{\mathbf{y}}) + \pi_0 (\mathbf{f}^\top \hat{\mathbf{y}} - \hat{\boldsymbol{\eta}}). \quad (22)$$

We first note the following correspondence between normalized distance functions and normalized separation problems, which sheds light on the role and desirable properties of the normalization function g , and paves the way for reformulating the separation problems. It operates by generalizing the Charnes-Cooper transformation (Charnes and Cooper 1962) for linear-fractional programs.

Proposition 9. Let $d_g(\hat{\mathbf{y}}, \hat{\boldsymbol{\eta}} | \boldsymbol{\pi}, \pi_0) = \frac{\boldsymbol{\pi}^\top (\mathbf{b} - B\hat{\mathbf{y}}) + \pi_0 (\mathbf{f}^\top \hat{\mathbf{y}} - \hat{\boldsymbol{\eta}})}{g(\boldsymbol{\pi}, \pi_0)}$ be a normalized distance function. Then, the separation problem (21) is equivalent to the normalized separation problem (22). That is,

$$d_g^*(\hat{\mathbf{y}}, \hat{\boldsymbol{\eta}}) = \max_{(\boldsymbol{\pi}, \pi_0) \in \Pi_g} \boldsymbol{\pi}^\top (\mathbf{b} - B\hat{\mathbf{y}}) + \pi_0 (\mathbf{f}^\top \hat{\mathbf{y}} - \hat{\boldsymbol{\eta}}).$$

Additionally, $g(\boldsymbol{\pi}, \pi_0) \leq 1$ is binding at optimality.

From a polyhedral perspective, Proposition 9 shows the equivalence between choosing a distance function and truncating the cone Π with a specific normalization function. Note that all general norms (including the ℓ_p -norms introduced in Section 2.2) are normalization functions. Figure 3(a) illustrates the effect of ℓ_1 -, ℓ_2 - and ℓ_∞ -norms on truncating the cone Π .

From a computational point of view, Proposition 9 shows that, for convex g , BSP can be converted into a problem of optimizing a linear function over a convex set Π_g . Additionally, since Π_g does not depend on $(\mathbf{y}^{(t)}, \boldsymbol{\eta}^{(t)})$, one may leverage the reoptimization capabilities of the solver whenever possible. For instance, a certificate produced at iteration t of the BD algorithm can be used for warm starting the separation subproblem at iteration $t + 1$. In particular, a convex piece-wise linear function $g(\boldsymbol{\pi}, \pi_0)$ amounts to solving linear programs with different objective function coefficients at each iteration, thus can be reoptimized using a primal simplex method. We provide further details in Section 4.

Finally, as stated in Proposition 10 below, any normalized distance function induces a monotonic epigraph distance function.

Proposition 10. Normalized distance function d_g induces a monotonic epigraph distance function d_g^* for any normalization function g .

3.3 Distance-Based Benders Decomposition Algorithm

We present an overview of our proposed Benders decomposition algorithm based on general Benders distance functions in Algorithm 2. Theorem 3, below, establishes finite convergence of this algorithm

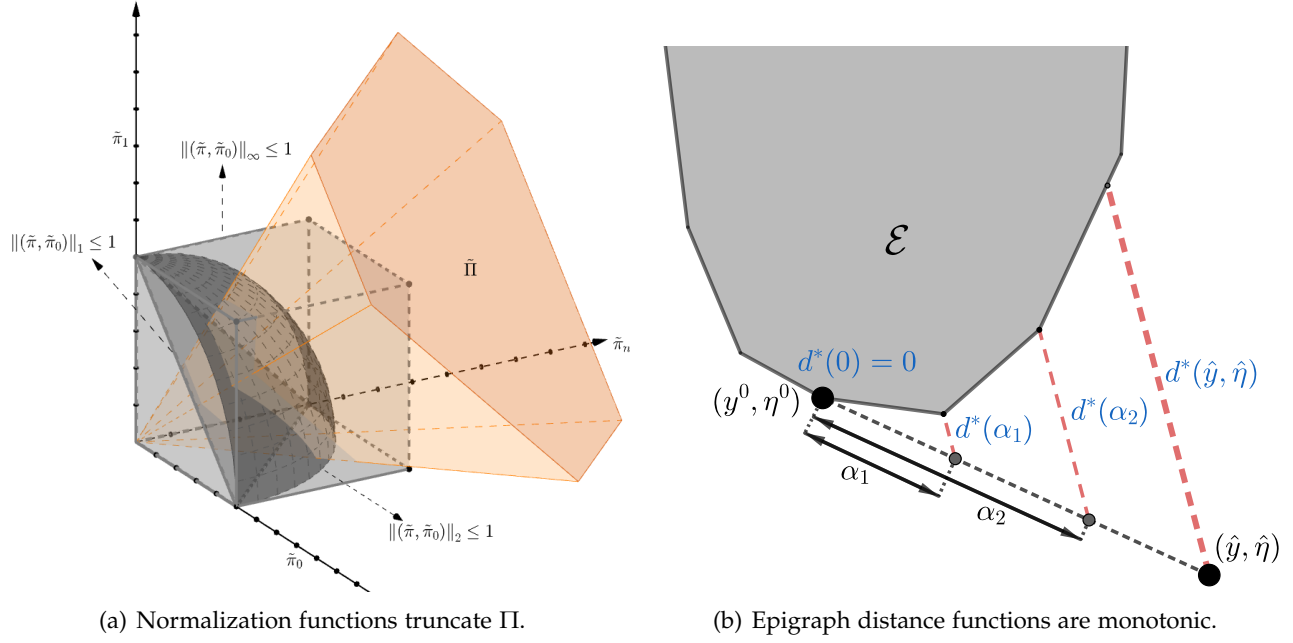


Figure 3: (a) Effect of ℓ_1 -norm (unit simplex), ℓ_2 -norm (sphere) and ℓ_∞ -norm (box) on truncating the cone Π . For illustration, the space of dual variables $(\pi, \pi_0) \in \Pi$ is transformed from \mathbb{R}^{m+1} to the \mathbb{R}^{n+1} -space via $(\tilde{\pi}, \tilde{\pi}_0) = (\pi_0 f^\top - \pi^\top B, \pi_0)$ and Π is mapped to this space as $\tilde{\Pi} = \{(\tilde{\pi}, \tilde{\pi}_0) \in \mathbb{R}^{n+1} : (\tilde{\pi}, \tilde{\pi}_0) = (\pi_0 f^\top - \pi^\top B, \pi_0), (\pi, \pi_0) \in \Pi\}$. (b) As we move away from the boundary of \mathcal{E} , d^* gets larger.

for a specific practical class of Benders distance function.

Theorem 3. *Let d_g be a Benders normalized distance function with a convex piece-wise linear normalization function g . Then BD Algorithm 2 converges to an optimal solution or asserts infeasibility of MP in a finite number of iterations.*

In particular, Algorithm 2 is finitely convergent when g is a linear function of (π, π_0) (see Section 4.2 for such linear functions) or when ℓ_1 - or ℓ_∞ -deepest cuts are produced. For other cases (e.g., Euclidean deepest cuts), one may choose to employ Euclidean deepest cuts in conjunction with known finitely convergent separation routines (e.g., classical BD cuts) to guarantee convergence while continuing to benefit from the desirable properties of deepest cuts.

Algorithm 2 Distance-Based Benders Decomposition Algorithm

- 1: Select a Benders distance function d .
 - 2: $t \leftarrow 1, \hat{\Pi}_t \leftarrow \emptyset$
 - 3: Solve MP with $\hat{\Pi}_t$ in place of Π and obtain master solution $(\mathbf{y}^{(t)}, \eta^{(t)})$.
 - 4: Solve BSP (21) to obtain $d^*(\mathbf{y}^{(t)}, \eta^{(t)})$ and the optimal solution $(\hat{\pi}, \hat{\pi}_0)$.
 - 5: **if** $d^*(\mathbf{y}^{(t)}, \eta^{(t)}) > 0$ **then**
 - 6: Set $\hat{\Pi}_{t+1} \leftarrow \hat{\Pi}_t \cup \{(\hat{\pi}, \hat{\pi}_0)\}$, $t \leftarrow t + 1$ and loop to Step 3.
 - 7: **else**
 - 8: Stop. $(\mathbf{y}^{(t)}, \eta^{(t)})$ is an optimal solution for MP with optimal value $\eta^{(t)}$.
 - 9: **end if**
-

4 Reformulations and Connections to other Cut Selection Strategies

In this section, we present some reformulations that may be used to implement distance-based cuts, as well as highlight special cases of normalized distance functions which link our concept of Benders distance function to other cut selection strategies in the literature. Section 4.1 begins by presenting reformulations of the separation problems introduced in Section 2, which can be used to computationally generate ℓ_p -deepest cuts using linear or quadratic programming solvers. Then, Section 4.2 considers the special case of normalized distance functions where the normalization function is linear, and examines how specific choices of linear coefficients correspond to cut selection strategies in the literature.

4.1 ℓ_p -deepest Cuts

We first show how SSP (18) can be cast as linear/quadratic programs using standard reformulation techniques. By homogeneity of ℓ_p -norms, using Proposition 9 we may restate SSP (18) as

$$\begin{aligned} \max_{(\boldsymbol{\pi}, \pi_0) \in \Pi} \quad & \boldsymbol{\pi}^\top (\mathbf{b} - B\hat{\mathbf{y}}) + \pi_0 (\mathbf{f}^\top \hat{\mathbf{y}} - \hat{\eta}) \\ \text{s.t.} \quad & \|(\pi_0 \mathbf{f}^\top - \boldsymbol{\pi}^\top B, \pi_0)\|_p \leq 1. \end{aligned} \tag{23}$$

Using this reformulation, we may express the constraint $\|(\pi_0 \mathbf{f}^\top - \boldsymbol{\pi}^\top B, \pi_0)\|_p \leq 1$ as a set of linear/quadratic constraints depending on the choice of p as follows.

- For $p = \infty$, we have $\|(\pi_0 \mathbf{f}^\top - \boldsymbol{\pi}^\top B, \pi_0)\|_\infty = \max \left\{ \pi_0, \max_{j=1, \dots, n} \{|\pi_0 f_j - \boldsymbol{\pi}^\top B_{.j}|\} \right\}$, where $B_{.j}$ is the j 'th column of matrix B . Therefore, $\|(\pi_0 \mathbf{f}^\top - \boldsymbol{\pi}^\top B, \pi_0)\|_\infty \leq 1$ can be represented by the $2n$ linear constraints $-1 \leq \pi_0 f_j - \boldsymbol{\pi}^\top B_{.j} \leq 1$ for each j , and a bound constraint $\pi_0 \leq 1$.
- For $p = 1$, we may rewrite $\|(\pi_0 \mathbf{f}^\top - \boldsymbol{\pi}^\top B, \pi_0)\|_1 = \pi_0 + \sum_{j=1}^n |\pi_0 f_j - \boldsymbol{\pi}^\top B_{.j}| \leq 1$ as $\pi_0 + \sum_{j=1}^n \tau_j \leq 1$ by introducing n new variables $\boldsymbol{\tau} \in \mathbb{R}_+^n$ and $2n$ constraints $-\tau_j \leq \pi_0 f_j - \boldsymbol{\pi}^\top B_{.j} \leq \tau_j$.
- For $p = 2$, one only needs to rewrite $\|(\pi_0 \mathbf{f}^\top - \boldsymbol{\pi}^\top B, \pi_0)\|_2 \leq 1$ as $\pi_0^2 + \sum_{j=1}^n (\pi_0 f_j - \boldsymbol{\pi}^\top B_{.j})^2 \leq 1$ to cast (23) as a convex quadratically constrained linear program.
- For $p > 2$ and integer, note that $\|(\pi_0 \mathbf{f}^\top - \boldsymbol{\pi}^\top B, \pi_0)\|_p \leq 1$ is equivalent to $\pi_0^p + \sum_{j=1}^n \tau_j^p \leq 1$, where $-\tau_j \leq \pi_0 f_j - \boldsymbol{\pi}^\top B_{.j} \leq \tau_j$. The constraint $\pi_0^p + \sum_{j=1}^n \tau_j^p \leq 1$ can be expressed as quadratic constraints using a series of transformations. For instance, with $p = 4$, it is not difficult to see that $\pi_0^4 + \sum_{j=1}^n \tau_j^4 \leq 1$ may be expressed using auxiliary variables $\{\beta_j\}_{j=0}^n$ as the following set of second-order constraints; similar transformations may be used for other values of p .

$$\beta_0^2 + \sum_{j=1}^n \beta_j^2 \leq 1, \quad \pi_0^2 \leq \beta_0, \quad \tau_j^2 \leq \beta_j \quad \forall j.$$

4.2 Linear Pseudonorms

Consider the class of normalization functions defined by choosing parameters (\boldsymbol{w}, w_0) such that $g(\boldsymbol{\pi}, \pi_0) = \boldsymbol{\pi}^\top \boldsymbol{w} + \pi_0 w_0 \geq 0$ for all $(\boldsymbol{\pi}, \pi_0) \in \Pi$. In this subsection, we study how different values of the (\boldsymbol{w}, w_0) parameters impact the resulting normalized Benders distance function, as well as how the cuts produced relate to other cut selection strategies in the literature. Note that a linear function g of this form satisfies most axioms of a norm; that is, g is subadditive (i.e., $g(\mathbf{u} + \mathbf{v}) \leq g(\mathbf{u}) + g(\mathbf{v})$), homogeneous (i.e., $g(\alpha \mathbf{u}) = \alpha g(\mathbf{u})$ for any $\alpha \geq 0$), and positive over Π , but not necessarily positive definite (i.e., $g(\boldsymbol{\pi}, \pi_0) = 0$ does not necessarily imply $(\boldsymbol{\pi}, \pi_0) = \mathbf{0}$, unless $(\boldsymbol{w}, w_0) > \mathbf{0}$). Hence, we call g a *linear*

pseudonorm over Π . With $g(\boldsymbol{\pi}, \pi_0) = \boldsymbol{\pi}^\top \boldsymbol{w} + \pi_0 w_0$, the separation problem (22) can be stated as the following linear program

$$\begin{aligned}
\max \quad & \boldsymbol{\pi}^\top (\boldsymbol{b} - B\hat{\boldsymbol{y}}) + \pi_0 (\boldsymbol{f}^\top \hat{\boldsymbol{y}} - \hat{\eta}) \\
\text{s.t.} \quad & \boldsymbol{\pi}^\top A \leq \pi_0 \boldsymbol{c}^\top \\
& \boldsymbol{\pi}^\top \boldsymbol{w} + \pi_0 w_0 = 1 \\
& \boldsymbol{\pi} \geq \mathbf{0}, \pi_0 \geq 0,
\end{aligned} \tag{24}$$

which contains only one additional variable and one additional constraint compared to DSP (5) in the classical BD algorithm. Note that the normalization constraint is an equality constraint since $g(\boldsymbol{\pi}, \pi_0)$ is binding at optimality.

Separation problem (24) is similar to the MIS (minimal infeasible subsystems) subproblem proposed by Fischetti et al. (2010). They derive the MIS subproblem by treating the separation problem as approximating the minimal source of infeasibility of FSP (11) by minimizing a positive linear function $\boldsymbol{\pi}^\top \boldsymbol{w} + \pi_0 w_0$ over the alternative polyhedron of Π (i.e., Π truncated by constraint $\boldsymbol{\pi}^\top (\boldsymbol{b} - B\hat{\boldsymbol{y}}) + \pi_0 (\boldsymbol{f}^\top \hat{\boldsymbol{y}} - \hat{\eta}) = 1$). Therefore, the MIS subproblem can be viewed as a special type of the Benders separation subproblem (21) in which the normalization function g takes the form of $g(\boldsymbol{\pi}, \pi_0) = \boldsymbol{\pi}^\top \boldsymbol{w} + \pi_0 w_0$.

As noted by Fischetti et al. (2010), the choice of the normalization coefficients (\boldsymbol{w}, w_0) can have a profound impact on the effectiveness of MIS cuts. In their implementation, the authors set $w_0 = 1$ and initially set $w_i = 1$, for all $i = 1, \dots, m$. They further suggest that setting $w_i = 0$ for the null rows of B (i.e., row i such that $B_{ij} = 0$ for all j) may lead to substantial improvement in the convergence of the BD algorithm. Below, we propose four ways for choosing parameters (\boldsymbol{w}, w_0) based on the parameters of the problem instance and discuss their implications and connections to other cut selection strategies.

4.2.1 Benders pseudonorm

A trivial choice for parameters \boldsymbol{w} and w_0 is to set $\boldsymbol{w} = \mathbf{0}$ and $w_0 = 1$, which leads to setting $\pi_0 = 1$, thus (24) reduces to the dual subproblem (5) in the classical BD algorithm. In other words, if we define $d_{\text{CB}}(\hat{\boldsymbol{y}}, \hat{\eta} | \boldsymbol{\pi}, \pi_0) = \frac{\boldsymbol{\pi}^\top (\boldsymbol{b} - B\hat{\boldsymbol{y}}) + \pi_0 (\boldsymbol{f}^\top \hat{\boldsymbol{y}} - \hat{\eta})}{\pi_0}$, as the classical Benders (CB) distance function, then

$$d_{\text{CB}}^*(\hat{\boldsymbol{y}}, \hat{\eta}) = \max_{(\boldsymbol{\pi}, \pi_0) \in \Pi} d_{\text{CB}}(\hat{\boldsymbol{y}}, \hat{\eta} | \boldsymbol{\pi}, \pi_0) = \tilde{Q}(\hat{\boldsymbol{y}}) + \boldsymbol{f}^\top \hat{\boldsymbol{y}} - \hat{\eta} = Q(\hat{\boldsymbol{y}}) - \hat{\eta}.$$

Therefore, as illustrated in Figure 1(b), $d_{\text{CB}}^*(\hat{\boldsymbol{y}}, \hat{\eta})$ can be geometrically interpreted as the distance from the point $(\hat{\boldsymbol{y}}, \hat{\eta})$ to the boundary of \mathcal{E} along the η -axis. Observe that, at iteration t of BD, $Q(\boldsymbol{y}^{(t)}) - \eta^{(t)} \geq UB - LB$, where $LB = \eta^{(t)}$ and UB is the best upper bound identified by the algorithm so far. Hence, $d_{\text{CB}}^*(\boldsymbol{y}^{(t)}, \eta^{(t)})$ estimates how far $(\boldsymbol{y}^{(t)}, \eta^{(t)})$ is from being optimal by overestimating the optimality gap. Thus, $d_{\text{CB}}^*(\boldsymbol{y}^{(t)}, \eta^{(t)}) = 0$ means $(\boldsymbol{y}^{(t)}, \eta^{(t)})$ is an optimal solution to (4), which is exactly the stopping criterion used in the classical BD algorithm.

4.2.2 Relaxed ℓ_1 pseudonorm

Expanding the ℓ_1 -norm as $\|(\pi_0 \boldsymbol{f}^\top - \boldsymbol{\pi}^\top B, \pi_0)\|_1 = \pi_0 + \sum_{j=1}^n |\pi_0 f_j - \boldsymbol{\pi}^\top B_{\cdot j}| = \pi_0 + \sum_{j=1}^n |\pi_0 f_j - \sum_{i=1}^m \pi_i B_{ij}|$ and using the triangle inequality, we obtain

$$\|(\pi_0 \boldsymbol{f}^\top - \boldsymbol{\pi}^\top B, \pi_0)\|_1 \leq \pi_0 (1 + \sum_{j=1}^n |f_j|) + \sum_{i=1}^m \pi_i \sum_{j=1}^n |B_{ij}|.$$

Hence, we refer to $g(\boldsymbol{\pi}, \pi_0) = \boldsymbol{\pi}^\top \boldsymbol{w} + \pi_0 w_0$ with $w_0 = 1 + \sum_{j=1}^n |f_j|$ and $w_i = \sum_{j=1}^n |B_{ij}|$ for $i = 1, \dots, m$ as the *relaxed ℓ_1 pseudonorm* (and write $R\ell_1$ for short). Note that, since $B_{ij} = 0$ for the null rows of B ,

$R\ell_1$ automatically sets $w_i = \sum_{j=1}^n |B_{ij}| = 0$ for the null rows of B , which is in line with the intuitive suggestion of Fischetti et al. (2010). Furthermore, observe that $d_{R\ell_1}$ defined as

$$d_{R\ell_1}(\hat{\mathbf{y}}, \hat{\eta} | \boldsymbol{\pi}, \pi_0) = \frac{\boldsymbol{\pi}^\top (\mathbf{b} - B\hat{\mathbf{y}}) + \pi_0 (\mathbf{f}^\top \hat{\mathbf{y}} - \hat{\eta})}{\boldsymbol{\pi}^\top \mathbf{w} + \pi_0 w_0}$$

underestimates d_{ℓ_1} . Thus, maximizing $d_{R\ell_1}$ serves as a surrogate for maximizing d_{ℓ_1} , but by solving a simpler LP. As stated in Proposition 11 below, the choice of (\mathbf{w}, w_0) according to $R\ell_1$ not only assigns meaningful values to the normalization parameters in the MIS subproblem, but also leads to a geometric interpretation of the MIS subproblem.

Proposition 11. *The following relationship between the epigraph distance functions induced by d_{CB} , d_{ℓ_p} , and $d_{R\ell_1}$ holds:*

$$d_{CB}^*(\hat{\mathbf{y}}, \hat{\eta}) = Q(\hat{\mathbf{y}}) - \hat{\eta} \geq d_{\ell_\infty}^*(\hat{\mathbf{y}}, \hat{\eta}) \geq \cdots \geq d_{\ell_p}^*(\hat{\mathbf{y}}, \hat{\eta}) \geq \cdots \geq d_{\ell_1}^*(\hat{\mathbf{y}}, \hat{\eta}) \geq d_{R\ell_1}^*(\hat{\mathbf{y}}, \hat{\eta}).$$

4.2.3 Magnanti-Wong-Papadakos pseudonorm

The Magnanti-Wong procedure for producing a Pareto-optimal cut using a given core point $\bar{\mathbf{y}}$ (i.e., $\bar{\mathbf{y}} \in \text{relint}(Y)$) involves solving the following subproblem (Magnanti and Wong 1981):

$$\max \left\{ \mathbf{u}^\top (\mathbf{b} - B\bar{\mathbf{y}}) : \mathbf{u}^\top (\mathbf{b} - B\hat{\mathbf{y}}) = \tilde{Q}(\hat{\mathbf{y}}), \mathbf{u} \in \mathcal{U} \right\}, \quad (25)$$

where $\mathcal{U} = \{\mathbf{u} \geq \mathbf{0} : \mathbf{u}^\top A \leq \mathbf{c}^\top\}$ and $\tilde{Q}(\hat{\mathbf{y}})$ is obtained by solving DSP (5). The constraint $\mathbf{u}^\top (\mathbf{b} - B\hat{\mathbf{y}}) = \tilde{Q}(\hat{\mathbf{y}})$ in (25) is imposed to guarantee that the dual solution \mathbf{u} is one of the alternative optimal solutions of the DSP induced by $\hat{\mathbf{y}}$. However, as noted by Papadakos (2008), one can still produce a Pareto-optimal cut by suppressing this constraint and solving

$$\tilde{Q}(\bar{\mathbf{y}}) = \max \left\{ \mathbf{u}^\top (\mathbf{b} - B\bar{\mathbf{y}}) : \mathbf{u} \in \mathcal{U} \right\}. \quad (26)$$

Note that $\tilde{Q}(\bar{\mathbf{y}}) - \mathbf{u}^\top (\mathbf{b} - B\bar{\mathbf{y}}) \geq 0$ for any $\mathbf{u} \in \mathcal{U}$, and problem (26) is equivalent to minimizing $\tilde{Q}(\bar{\mathbf{y}}) - \mathbf{u}^\top (\mathbf{b} - B\bar{\mathbf{y}})$. Additionally, $\frac{\pi}{\pi_0} \in \mathcal{U}$ for any $(\boldsymbol{\pi}, \pi_0) \in \Pi$ such that $\pi_0 > 0$. Consequently, one can approximate a Pareto-optimal cut when cutting off the point $(\hat{\mathbf{y}}, \hat{\eta})$ by employing

$$d_{\text{MWP}}(\hat{\mathbf{y}}, \hat{\eta} | \boldsymbol{\pi}, \pi_0) = \frac{\boldsymbol{\pi}^\top (\mathbf{b} - B\hat{\mathbf{y}}) + \pi_0 (\mathbf{f}^\top \hat{\mathbf{y}} - \hat{\eta})}{\pi_0 \tilde{Q}(\bar{\mathbf{y}}) - \boldsymbol{\pi}^\top (\mathbf{b} - B\bar{\mathbf{y}})},$$

as the distance function, which is equivalent to setting $g(\boldsymbol{\pi}, \pi_0) = \boldsymbol{\pi}^\top \mathbf{w} + \pi_0 w_0$ with $(\mathbf{w}, w_0) = (B\bar{\mathbf{y}} - \mathbf{b}, \tilde{Q}(\bar{\mathbf{y}}))$. We refer to $g(\boldsymbol{\pi}, \pi_0)$ with this choice of (\mathbf{w}, w_0) as the *Magnanti-Wong-Papadakos (MWP) pseudonorm*, which further connects the distance functions to this well-known cut selection strategy. Note that $\tilde{Q}(\bar{\mathbf{y}})$ needs to be computed only once and that the normalization function remains the same in the course of BD Algorithm 2.

4.2.4 Conforti-Wolsey pseudonorm

Recently, Conforti and Wolsey (2019) proposed an interesting procedure for producing facet-defining cuts using a core point. Given a core point $\bar{\mathbf{y}}$ and its optimal value $Q(\bar{\mathbf{y}}) = \tilde{Q}(\bar{\mathbf{y}}) + \mathbf{f}^\top \bar{\mathbf{y}}$, the geometric interpretation of this idea is to find the closest point to $(\hat{\mathbf{y}}, \hat{\eta})$ on the line segment between $(\bar{\mathbf{y}}, Q(\bar{\mathbf{y}}))$ and $(\hat{\mathbf{y}}, \hat{\eta})$ that renders FSP (11) feasible. In our context, their procedure translates to solving

$$\begin{aligned} \min \quad & \lambda \\ \text{s.t.} \quad & -\mathbf{c}^\top \mathbf{x} + \lambda \left(Q(\bar{\mathbf{y}}) - \hat{\eta} - \mathbf{f}^\top (\bar{\mathbf{y}} - \hat{\mathbf{y}}) \right) \geq -\hat{\eta} + \mathbf{f}^\top \hat{\mathbf{y}} \\ & A\mathbf{x} + \lambda B(\bar{\mathbf{y}} - \hat{\mathbf{y}}) \geq \mathbf{b} - B\hat{\mathbf{y}} \\ & \mathbf{x} \geq \mathbf{0}, 1 \geq \lambda \geq 0. \end{aligned} \quad (27)$$

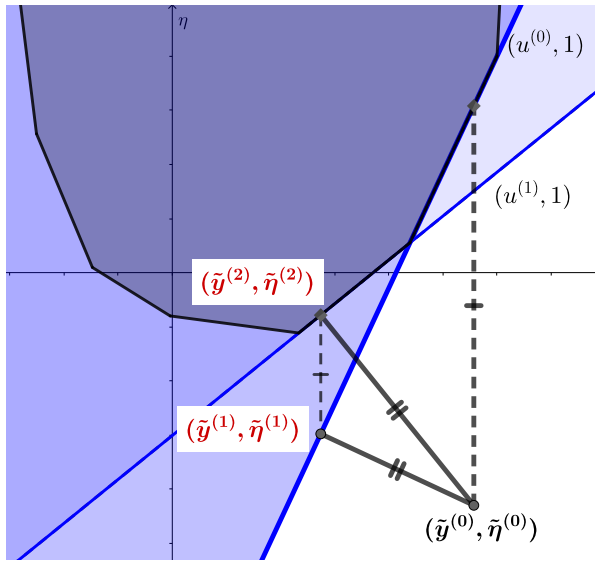


Figure 4: Guided projections algorithm. $(\tilde{\mathbf{y}}^{(0)}, \tilde{\eta}^{(0)}) = (\hat{\mathbf{y}}, \hat{\eta})$ is the point to be separated, $(\tilde{\mathbf{y}}^{(2)}, \tilde{\eta}^{(2)})$ is its projection onto \mathcal{E} (dark polygon), and $(\mathbf{u}^{(1)}, 1)$ corresponds to the deepest cut. To find this projection and the deepest cut, we first obtain the optimality cut defined by $\mathbf{u}^{(0)}$ by solving a classical DSP induced by $\tilde{\mathbf{y}}^{(0)} = \hat{\mathbf{y}}$. We then find the projection of $(\hat{\mathbf{y}}, \hat{\eta})$ onto this half-space to obtain $(\tilde{\mathbf{y}}^{(1)}, \tilde{\eta}^{(1)})$. Repeating this procedure for another step produces dual solution $(\mathbf{u}^{(1)}, 1)$ and primal solution $(\tilde{\mathbf{y}}^{(2)}, \tilde{\eta}^{(2)})$.

First, note that we may suppress $\lambda \leq 1$ since $(\bar{\mathbf{y}}, Q(\bar{\mathbf{y}}))$ is feasible for FSP (11). Next, assigning dual variable π_0 to the first constraint and $\boldsymbol{\pi}$ to the second set of constraints, we may express (27) in its dual form as

$$\begin{aligned} \max \quad & \boldsymbol{\pi}^\top (\mathbf{b} - B\hat{\mathbf{y}}) + \pi_0 (\mathbf{f}^\top \hat{\mathbf{y}} - \hat{\eta}) \\ \text{s.t.} \quad & \boldsymbol{\pi}^\top B(\bar{\mathbf{y}} - \hat{\mathbf{y}}) + \pi_0 \left(Q(\bar{\mathbf{y}}) - \hat{\eta} - \mathbf{f}^\top (\bar{\mathbf{y}} - \hat{\mathbf{y}}) \right) \leq 1 \\ & (\boldsymbol{\pi}, \pi_0) \in \Pi, \end{aligned}$$

which is equivalent to employing $g(\boldsymbol{\pi}, \pi_0) = \boldsymbol{\pi}^\top \mathbf{w} + \pi_0 w_0$ in the normalized separation problem (22) with $w_0 = Q(\bar{\mathbf{y}}) - \hat{\eta} - \mathbf{f}^\top (\bar{\mathbf{y}} - \hat{\mathbf{y}})$ and $\mathbf{w} = B(\bar{\mathbf{y}} - \hat{\mathbf{y}})$. We refer to $g(\boldsymbol{\pi}, \pi_0)$ with this choice of (\mathbf{w}, w_0) as the *Conforti-Wolsey (CW) pseudonorm*. We remark that the coefficients of the CW pseudonorm change as $(\hat{\mathbf{y}}, \hat{\eta})$ changes; thus, unlike other normalization functions presented so far, one should update the normalization constraint for each new point being separated.

5 Guided Projections Algorithm for Producing ℓ_p -deepest Cuts

The reformulations previously presented in Section 4.1 may be used to produce ℓ_p -deepest cuts using LP/QP blackbox solvers. However, unless the subproblem happens to be small or can be decomposed into smaller subproblems, exploiting the combinatorial structure which otherwise would be present in classical Benders subproblems is not straightforward. Since exploiting combinatorial structure often produces an order of magnitude in speed-up for the BD algorithm, we propose in this section a specialized iterative algorithm that produces or approximates ℓ_p -deepest cuts through a series of projections guided by classical Benders cuts.

As noted in Proposition 1, we can express \mathcal{E} in terms of the classical optimality and feasibility cuts, which means deepest cuts can be represented as combination of these cuts. Provided that there exists an oracle for producing classical cuts efficiently, we show how these cuts can be used for producing

deepest cuts. Recall from Theorem 1 that producing an ℓ_p -deepest cut is equivalent to finding the ℓ_q -projection of the incumbent point $(\hat{\mathbf{y}}, \hat{\eta})$ onto the epigraph \mathcal{E} . Instead of finding this projection directly, we can iteratively *guide* the projection, as illustrated in Figure 4, by moving from the incumbent point to its projection on the epigraph by successively identifying facets of the epigraph using classical Benders dual subproblems; thus, we call this iterative procedure the *Guided Projections Algorithm* (GPA). GPA separates the projection problem (19) into two simpler problems in a row generation manner: (a) producing a new facet of \mathcal{E} using classical Benders subproblems, and (b) projecting the incumbent point $(\hat{\mathbf{y}}, \hat{\eta})$ onto these half-spaces.

Algorithm 3 provides an overview of GPA. Starting with $\mathcal{C}^{(0)}$ as an initial approximation of \mathcal{E} , GPA first projects $(\hat{\mathbf{y}}, \hat{\eta})$ onto $\mathcal{C}^{(0)}$ to obtain the intermediate projection $(\tilde{\mathbf{y}}^{(0)}, \tilde{\eta}^{(0)})$. GPA then produces a classical cut by solving DSP evaluated at $\tilde{\mathbf{y}}^{(0)}$, and adds the cut to $\mathcal{C}^{(0)}$ to obtain $\mathcal{C}^{(1)}$. GPA then iterates by updating the epigraph approximation and producing new dual solutions. Note that at iteration h , given the intermediate projection $(\tilde{\mathbf{y}}^{(h)}, \tilde{\eta}^{(h)})$, the values of $\|(\hat{\mathbf{y}}, \hat{\eta}) - (\tilde{\mathbf{y}}^{(h)}, \tilde{\eta}^{(h)})\|_q$ and $\|(\hat{\mathbf{y}}, \hat{\eta}) - (\tilde{\mathbf{y}}^{(h)}, Q(\tilde{\mathbf{y}}^{(h)}))\|_q$ provide lower- and upper-bounds on $d_{\ell_p}^*(\hat{\mathbf{y}}, \hat{\eta})$ (i.e., the ℓ_q distance from $(\hat{\mathbf{y}}, \hat{\eta})$ to \mathcal{E}), respectively. As the algorithm iterates and $\mathcal{C}^{(h)}$ becomes a tighter approximation of \mathcal{E} , these bounds converge; thus, the intermediate projections converge to the projection of $(\hat{\mathbf{y}}, \hat{\eta})$ onto \mathcal{E} .

Once GPA converges, we obtain a sequence of dual solutions $\{(\boldsymbol{\pi}^{(h)}, \pi_0^{(h)})\}$, and by construction, each one of these solutions can be used for separating $(\hat{\mathbf{y}}, \hat{\eta})$ from \mathcal{E} . Note that the dual solution associated with the deepest cut might not be one of these solutions, but a convex combination of them. Therefore, one can choose to add one or more of the cuts produced by GPA to the BD master problem. Note that GPA guarantees convergence of the BD algorithm, even if we terminate GPA before converging to the true projection. This is because the cut obtained in the first iteration of this algorithm is the cut that one would produce using the classical BD algorithm.

We remark that $\mathcal{C}^{(0)}$ need not be initialized with an empty set, and the algorithm may benefit from initializing $\mathcal{C}^{(0)}$ with a few simple constraints. For instance, one can use the cuts generated before (e.g., in separating master solutions in the previous iterations of BD) to initialize $\mathcal{C}^{(0)}$. Also, in many cases the constraints that define Y are also feasibility cuts. For instance, the non-negativity constraints $\mathbf{y} \geq \mathbf{0}$ are necessary to ensure boundedness in DSP for facility location-type problems. Therefore, one can add such constraints to $\mathcal{C}^{(0)}$ as well.

6 Computational Experiments

In this section, we first provide details for the effective implementation of the BD algorithm in general as well as details specific to our approach. We then compare the performance of deepest cuts and other variants of Benders cuts on instances of the capacitated facility location problem (CFLP), whose structure is known to be well-suited for BD (Fischetti et al. 2016, 2017).

6.1 Implementation Details

We conducted our computational study on a Dell desktop equipped with Intel(R) Xeon(R) CPU E5-2680 v3 at 2.50GHz with 8 Cores and 32 GB of memory running a 64-bit Windows 10 operating system. We coded our algorithms in C# and solved the linear/quadratic problems using the ILOG Concert library and CPLEX 12.10 solver. In the following, we provide general implementation details for BD, which we believe are of technical value beyond the application of this paper.

Algorithm 3 Guided Projections Algorithm

- 1: **STEP 0:** Initialize $\mathcal{C}^{(0)} \leftarrow \emptyset$, $h \leftarrow 0$;
- 2: **while** not converged **do**
- 3: **STEP 1 (Projection):** If $h = 0$, set $(\hat{\mathbf{y}}^{(h)}, \hat{\eta}^{(h)}) = (\hat{\mathbf{y}}, \hat{\eta})$. Otherwise, find the ℓ_q -projection of $(\hat{\mathbf{y}}, \hat{\eta})$ onto $\mathcal{C}^{(h)}$, and let $(\tilde{\mathbf{y}}^{(h)}, \tilde{\eta}^{(h)})$ be this projection.

$$(\tilde{\mathbf{y}}^{(h)}, \tilde{\eta}^{(h)}) \leftarrow \underset{(\mathbf{y}, \eta) \in \mathcal{C}^{(h)}}{\operatorname{argmin}} \quad \|(\mathbf{y} - \hat{\mathbf{y}}, \eta - \hat{\eta})\|_q \quad (28)$$

- 4: **STEP 2 (Cut Generation):** Solve the following classical DSP:

$$[\text{DSP}] \quad \tilde{Q}(\tilde{\mathbf{y}}^{(h)}) = \max \left\{ \mathbf{u}^\top (\mathbf{b} - B\tilde{\mathbf{y}}^{(h)}) : \mathbf{u}^\top A \leq c, \mathbf{u} \geq \mathbf{0} \right\}.$$

- 5: **if** DSP is bounded **then**
 - 6: Let $\mathbf{u}^{(h)}$ be an optimal solution to DSP and set $(\boldsymbol{\pi}^{(h)}, \pi_0^{(h)}) \leftarrow (\mathbf{u}^{(h)}, 1)$
 - 7: **else**
 - 8: Let $\mathbf{v}^{(h)}$ be an optimal ray to DSP and set $(\boldsymbol{\pi}^{(h)}, \pi_0^{(h)}) \leftarrow (\mathbf{v}^{(h)}, 0)$
 - 9: **end if**
 - 10: **STEP 3 (Epigraph Approximation):** $\mathcal{C}^{(h+1)} \leftarrow \mathcal{C}^{(h)} \cap \mathcal{H}(\boldsymbol{\pi}^{(h)}, \pi_0^{(h)})$
 - 11: $h \leftarrow h + 1$
 - 12: **end while**
-

6.1.1 Modern implementation of BD algorithm

While the sequential implementations of BD Algorithms 1 or 2 may appear intuitive, they come with several limitations. Of note, building a new branch-and-bound tree from scratch at each iteration incurs a large amount of overhead, especially when several iterations of the BD algorithm are needed. Moreover, at each iteration, only the optimal integer solution to the master problem is provided to the separation problems. This in turn may ignore several integer feasible solutions that are encountered during the branch-and-bound search, which are potentially optimal for the original problem but sub-optimal for the current iteration. This also ignores fractional solutions, which may prove useful for producing effective Benders cuts.

An alternative is to implement BD algorithms in the modern fashion, known as Branch-and-Benders-Cut (BBC), where Benders cuts are added to the cut pool of branch-and-cut on the fly (see e.g., Fortz and Poss 2009, for one of the early implementations of BBC). BBC allows for solving the integer master problem in a single run, thus potentially saving computation time by avoiding solving multiple integer master problems. Furthermore, this framework permits separating both integer and fractional master solutions. The former is implemented by treating BD cuts as lazy constraints, while the latter is implemented by treating BD cuts as valid inequalities for the master problem, which are invoked by CPLEX using the `LazyConstraint` callback when the current-node solution happens to be integer and `UserCut` callback at each branch decision node, respectively.

6.1.2 Scaling of η in the cuts and normalization functions

A pitfall in implementing BD is that scales of master problem variables η and \mathbf{y} are often unbalanced, meaning that the coefficient of η in (optimality) cuts is often too small or too large compared to the coefficients of the \mathbf{y} variables. This imbalance poses two numerical issues:

- (i) The cuts become numerically unstable and the solver may not handle them correctly, which in turn may result in having to cut off (almost) the same point over and over.

(ii) Note that, in the cut $\boldsymbol{\pi}^\top \mathbf{b} \leq (\boldsymbol{\pi}^\top B - \pi_0 \mathbf{f}^\top) \mathbf{y} + \pi_0 \eta$, the coefficient of η is π_0 , while the coefficient of \mathbf{y} is $\boldsymbol{\pi}^\top B - \pi_0 \mathbf{f}^\top$. Therefore, an imbalanced cut implies an imbalanced normalization function $g(\boldsymbol{\pi}, \pi_0) = \|\boldsymbol{\pi}^\top B - \pi_0 \mathbf{f}^\top, \pi_0\|_p$ in the ℓ_p -distance function (17), which poses numerical issues in the separation problem (18).

To resolve this issue, we replace η in the master problem (10) with $\eta = \beta\gamma$ for some suitably-chosen scaling factor $\beta > 0$. Consequently, γ becomes the decision variable in place of η , and we minimize γ in the objective function of (10). Note that, for a given $(\boldsymbol{\pi}, \pi_0) \in \Pi$, the cut becomes

$$\boldsymbol{\pi}^\top \mathbf{b} \leq (\boldsymbol{\pi}^\top B - \pi_0 \mathbf{f}^\top) \mathbf{y} + \beta \pi_0 \gamma.$$

Consequently, the ℓ_p -norm normalization function in (17) becomes

$$g(\boldsymbol{\pi}, \pi_0) = \|\boldsymbol{\pi}^\top B - \pi_0 \mathbf{f}^\top, \beta \pi_0\|_p,$$

and the relaxed ℓ_1 -normalization function is obtained accordingly. Note that if we replace $\eta = \beta\gamma$, the scaling must be reflected in the primal space as well, and the projection problems must be done in the space of \mathbf{y} and γ . For instance, the projection problem (28) at iteration h of GPA becomes

$$(\tilde{\mathbf{y}}^{(h)}, \tilde{\gamma}^{(h)}) \leftarrow \underset{(\mathbf{y}, \gamma) \in \mathcal{C}^{(h)}}{\operatorname{argmin}} \quad \|(\mathbf{y} - \hat{\mathbf{y}}, \gamma - \hat{\gamma})\|_q.$$

From the projection perspective, it is not difficult to see that if β is too large, \mathbf{y} becomes the dominant component in the projection (particularly for small values of q , e.g., $q = 1$), causing deepest cuts to converge to classical Benders cuts. To choose a suitable value for β , we first solve DSP (26) using a core point $\bar{\mathbf{y}}$ to obtain the dual solution $(\hat{\mathbf{u}}, 1)$ and the optimality cut $\eta + (\hat{\mathbf{u}}^\top B - \mathbf{f}^\top) \mathbf{y} \geq \hat{\mathbf{u}}^\top \mathbf{b}$. We then set β as

$$\beta = \frac{1}{n} \|\hat{\mathbf{u}}^\top B - \mathbf{f}^\top\|_1,$$

which is the average absolute coefficient value of the \mathbf{y} variables in the cut. Note that we choose β only once in the course of BD Algorithm 2, and use the same β for stabilizing all cuts.

6.1.3 Reoptimizing the separation subproblems

Another important aspect in implementing the BD algorithm is being able to reoptimize the separation problems and retrieving the cuts quickly when a solver is used for solving the separation subproblems. Note that only the objective function in the separation problem (22) changes from one iteration of the BD algorithm 2 to another. For linear separation subproblems, one can use the primal simplex algorithm by setting parameter `Cplex.Param.RootAlgorithm` to `Cplex.Algorithm.Primal` to leverage the reoptimization capabilities of this method.

Additionally, at iteration t of BD algorithm, rearranging the objective function in (22) as

$$\boldsymbol{\pi}^\top \mathbf{b} - \sum_{j=1}^n (\boldsymbol{\pi}^\top B_{\cdot j} - \pi_0 f_j) y_j^{(t)} - \pi_0 \eta^{(t)},$$

note that one needs to update the coefficient of $\boldsymbol{\pi}^\top B_{\cdot j} - \pi_0 f_j$ (i.e., $y_j^{(t)}$) only when $y_j^{(t)} \neq y_j^{(t-1)}$. Therefore, we may additionally define n auxiliary variables $\tau_j = \boldsymbol{\pi}^\top B_{\cdot j} - \pi_0 f_j$ to avoid changing the coefficients of all dual variables in the separation subproblems. For instance, the separation problem (23) for producing ℓ_p -deepest cuts becomes

$$\max \left\{ \boldsymbol{\pi}^\top \mathbf{b} - \boldsymbol{\tau} \hat{\mathbf{y}} - \pi_0 \hat{\eta} : \|(\boldsymbol{\tau}, \pi_0)\|_p \leq 1, \boldsymbol{\tau} = \boldsymbol{\pi}^\top B - \pi_0 \mathbf{f}^\top, (\boldsymbol{\pi}, \pi_0) \in \Pi \right\}.$$

The τ variables also simplify the expression for the normalization constraint (e.g., in ℓ_p -norm or in CW). Moreover, after the subproblem is solved, one can save $\mathcal{O}(mn)$ arithmetic operations in computing the cut coefficients by easily retrieving the value of the τ variables from the solver without having to recalculate the coefficients based on the π variables.

6.2 Benchmark Instances

We used instances of the CFLP as a testbed for evaluating the performance of the BD algorithm with different choices of distance functions. Facility location problems lie at the heart of network design and planning, and arise naturally in a wide range of applications such as supply chain management, telecommunications systems, urban transportation planning, health care systems and humanitarian logistics to count a few (see e.g., Drezner and Hamacher 2001). Given a set of customers and a set of potential locations for the facilities, CFLP in its simplest form as formulated below, consists of determining which facilities to open and how to assign customers to opened facilities to minimize cost, i.e.,

$$\min \sum_{l=1}^k \sum_{j=1}^n x_{lj} d_l c_{lj} + \sum_{j=1}^n f_j y_j \quad (29)$$

$$\text{s.t.} \quad \sum_{j=1}^n x_{lj} \geq 1 \quad \forall l \quad (30)$$

$$\sum_{l=1}^k x_{lj} d_l \leq s_j y_j \quad \forall j \quad (31)$$

$$x_{lj} \leq y_j \quad \forall l, j \quad (32)$$

$$\mathbf{x} \geq \mathbf{0}, \mathbf{y} \in Y, \quad (33)$$

where f_j and s_j are respectively the installation cost and capacity of facility $j = 1, \dots, n$; d_l is the demand of customer $l = 1, \dots, k$; c_{lj} is the cost of serving one unit of demand from customer l using facility j ; and $Y = \{\mathbf{y} \in \{0, 1\}^n : \sum_{l=1}^k d_l \leq \sum_{j=1}^n s_j y_j\}$ is the domain of the \mathbf{y} variables.

We used two sets of benchmark instances from the literature:

CAP: The famous CAP data set from the OR-Library (Beasley 2021) consists of 24 small instances with $k = 50$ customers and $n \in \{16, 25, 50\}$ facilities, and 12 large instances with $n = 100$ facilities and $k = 1000$ customers. The instances are denoted CAPx1–CAPx4, where $x \in \{6, 7, 9, 10, 12, 13\}$ for the small instances and $x \in \{a, b, c\}$ for the large instances.

CST: These are instances that we randomly generated following the procedure proposed by Cornuéjols et al. (1991). We denote each instance by tuple (n, k, r) , where (n, k) pairs were selected from $\{(50, 50), (50, 100), (100, 100), (100, 200), (100, 500), (500, 500), (100, 1000), (200, 1000), (500, 1000), (1000, 1000)\}$ and the scaling factor r was selected from $\{5, 10, 15, 20\}$. For each choice of (n, k, r) we randomly generated 4 instances as follows. For each facility $j \in \{1, \dots, n\}$, we randomly drew s_j and f_j from $U[10, 160]$ and $U[0, 90] + U[100, 110] \sqrt{s_j}$, respectively, where $U[a, b]$ represents the uniform distribution on $[a, b]$. For each customer $l \in \{1, \dots, k\}$, we randomly drew d_l from $U[5, 35]$. Finally, we scaled the facility capacities using parameter r such that $r = \sum_{j=1}^n s_j / \sum_{l=1}^k d_l$. To compute the allocation costs, we placed the customers and facilities in a unit square uniformly at random, and set c_{lj} to 10 times the Euclidean distance of facility j from customer l .

We remark that, whenever a core point $\bar{\mathbf{y}}$ was needed (e.g., for the MWP and CW pseudonorms) we chose the core point by setting $\bar{y}_j = 1/r + \epsilon$ for each j , where $\epsilon = 10^{-3}$ and $r = \sum_{j=1}^n s_j / \sum_{l=1}^k d_l$. The same core point was used for choosing β for scaling the η variable as described in Section 6.1.2.

6.3 Numerical Results for Standard Reformulations

We start by presenting numerical results for distance-based BD algorithms where the separation problems are reformulated as LP/QP programs using standard transformation techniques presented in Section 4 and solved using a solver without exploiting any combinatorial structures in the problem instances. We considered nine cut selection strategies:

- ℓ_1 and ℓ_∞ : Deepest cuts with ℓ_1 and ℓ_∞ norms on the coefficients. Separation problems are transformed into linear programs according to the transformations given in Section 4.1.
- ℓ_2 and ℓ_4 : Deepest cuts with ℓ_2 and ℓ_4 norms on the coefficients. Separation problems are transformed into quadratic programs according to the transformations given in Section 4.1.
- **MIS**: Distance function with linear normalization function $g(\boldsymbol{\pi}, \pi_0) = \boldsymbol{w}^\top \boldsymbol{\pi} + w_0 \pi_0$, with (\boldsymbol{w}, w_0) in the MIS subproblem chosen according to the default setting suggested by Fischetti et al. (2010), that is $w_0 = 1$, $w_i = 0$ if the i 'th row of B is all zeros and $w_i = 1$ otherwise.
- **$R\ell_1$** : Distance function with linear normalization function $g(\boldsymbol{\pi}, \pi_0) = \boldsymbol{w}^\top \boldsymbol{\pi} + w_0 \pi_0$, with (\boldsymbol{w}, w_0) in the MIS subproblem chosen according to $R\ell_1$ as described in Section 4.2.2.
- **MWP**: Distance function with linear normalization function $g(\boldsymbol{\pi}, \pi_0) = \boldsymbol{w}^\top \boldsymbol{\pi} + w_0 \pi_0$, with (\boldsymbol{w}, w_0) in the MIS subproblem chosen according to MWP as described in Section 4.2.3.
- **CW**: Distance function with linear normalization function $g(\boldsymbol{\pi}, \pi_0) = \boldsymbol{w}^\top \boldsymbol{\pi} + w_0 \pi_0$, with (\boldsymbol{w}, w_0) in the MIS subproblem chosen according to CW as described in Section 4.2.4.
- **CB**: Classical Benders cuts which correspond to setting $g(\boldsymbol{\pi}, \pi_0) = \pi_0$.

Instance	Cuts									Time (sec.)								
	CB	MIS	MWP	CW	$R\ell_1$	ℓ_1	ℓ_∞	ℓ_2	ℓ_4	CB	MIS	MWP	CW	$R\ell_1$	ℓ_1	ℓ_∞	ℓ_2	ℓ_4
CAP6* (16,50)	17.5	48.0	10.3	30.0	18.8	7.3	13.8	10.3	54.8	0.04	0.26	0.08	0.72	0.08	0.20	0.08	4.75	19.11
CAP7* (16,50)	15.0	383.5	10.3	13.3	12.3	5.5	10.3	8.3	34.3	0.02	0.98	0.05	0.15	0.03	0.11	0.05	3.57	10.28
CAP9* (25,50)	44.8	482.3	21.5	30.0	64.5	8.3	16.8	9.8	136.3	0.14	2.44	0.20	0.59	0.36	0.56	0.26	7.99	84.39
CAP10* (25,50)	29.3	3363.0	11.5	19.8	43.0	7.3	24.8	11.5	82.8	0.05	127.98	0.10	0.32	0.16	0.28	0.17	9.44	39.32
CAP12* (50,50)	125.8	5449.5	36.0	37.8	120.8	14.0	88.3	21.3	21.0	0.92	384.22	0.90	1.94	1.84	2.97	3.96	84.33	13.05
CAP13* (50,50)	103.3	6626.0	23.0	29.3	61.8	9.0	60.3	27.8	39.8	0.36	384.14	0.52	1.18	0.64	1.45	1.23	85.93	19.89
Mean	55.9	2725.4	18.8	26.7	53.5	8.6	35.7	14.8	61.5	0.25	150.00	0.31	0.82	0.52	0.93	0.96	32.67	31.01
CST (50,50,5)	17.8	12.0	19.0	5.8	5.0	4.3	4.0	4.3	6.5	0.09	0.23	0.50	0.23	0.14	0.61	0.34	6.19	3.32
CST (50,50,10)	19.3	11.8	15.0	7.5	3.5	4.0	3.5	4.0	6.8	0.18	0.70	0.48	0.28	0.23	0.54	0.25	5.77	3.94
CST (50,50,15)	5.5	5.5	15.8	3.5	2.8	3.0	1.8	2.8	3.8	0.03	0.25	0.59	0.25	0.28	0.34	0.18	3.29	1.96
CST (50,50,20)	9.0	8.0	18.5	7.5	4.8	5.5	4.5	5.5	7.5	0.07	0.47	0.77	0.31	0.44	0.87	0.34	8.20	4.52
CST (50,100,5)	20.8	14.3	20.3	6.5	6.0	7.0	4.8	6.0	8.8	0.34	1.82	1.45	0.70	0.61	2.54	0.85	3.03	8.00
CST (50,100,10)	28.0	17.8	18.3	6.5	4.3	9.3	6.3	9.3	7.0	0.61	4.38	1.89	0.91	0.85	3.79	1.55	4.55	6.85
CST (50,100,15)	7.5	4.8	13.5	2.5	2.8	2.8	2.0	3.0	4.0	0.16	0.75	2.11	0.68	0.66	1.01	0.69	1.40	4.36
CST (50,100,20)	20.3	13.0	25.0	7.0	5.5	7.5	5.8	7.5	9.8	0.52	5.83	4.35	1.36	2.53	4.46	1.46	3.85	10.06
CST (100,100,5)	8.3	7.3	12.8	5.0	1.8	3.3	3.0	3.3	8.5	0.20	0.79	1.75	1.64	1.38	4.16	1.39	7.11	12.99
CST (100,100,10)	33.5	13.0	19.3	7.8	6.3	6.5	6.8	7.5	11.0	2.01	1.19	4.29	1.70	3.35	10.49	3.22	14.75	17.23
CST (100,100,15)	43.5	17.3	26.5	8.3	5.3	11.3	7.0	7.5	10.5	3.64	22.30	8.49	3.34	4.62	25.56	3.35	13.49	17.37
CST (100,100,20)	38.8	13.5	25.0	7.0	5.8	6.5	5.5	9.0	8.3	4.45	15.57	11.32	2.48	5.14	14.43	3.16	15.45	12.02
CST (100,200,5)	12.8	7.5	10.5	5.8	2.8	4.3	3.3	4.0	8.8	1.44	3.42	19.61	11.25	6.00	35.16	15.89	24.47	88.24
CST (100,200,10)	66.5	24.0	24.3	7.3	7.0	11.5	7.0	12.8	11.3	21.34	126.52	25.57	9.76	12.85	57.48	11.51	61.98	102.33
CST (100,200,15)	46.3	37.7	30.3	5.8	8.3	12.7	9.0	11.5	16.5	35.88	520.30	43.14	8.28	22.83	163.59	14.81	45.43	141.73
CST (100,200,20)	62.7	30.8	25.3	5.5	7.0	14.5	8.0	12.7	17.3	25.91	450.67	46.81	7.04	26.33	125.50	12.02	58.17	167.40
Mean	27.5	14.9	19.9	6.2	4.9	7.1	5.1	6.9	9.1	6.05	72.20	10.82	3.14	5.51	28.16	4.44	17.32	37.65

Table 1: Performance comparison of BD with different distance functions on CAP and CST instances. Separation problems are solved using a LP/QP solver without exploiting combinatorial structure.

Table 1 compares the computational performance of BD with different choices of the normalization functions across CAP and CST instances. Each row in Table 1 corresponds to the average performance metrics over four instances. The CAP instances are formatted as “CAPx* (n, k)”. For instance CAP6* (16,50) corresponds to CAP instances CAP61–CAP64, which contain $n = 16$ facilities and $k = 50$ customers. The CST instances are formatted as “CST (n, k, r)”, which correspond to four randomly generated instances with n facilities, k customers, and capacity/demand scaling factor r . In these experiments, we have used the small and moderately sized instances of these data sets (i.e., with at most $k = 200$ customers) to showcase the quality of the cuts produced based on each normalization function.

The results provided in Table 1 highlight the effectiveness of ℓ_p -deepest cuts in reducing the number of cuts compared to CB and MIS cuts with different choices of the normalization coefficients. This is particularly pronounced with $p = 1$ and $p = 2$ in CAP instances, while all choices of $p \in \{1, 2, 4, \infty\}$ perform well in CST instances. A surprising result is that the default choices of normalization coefficients in MIS suffers from producing weak cuts in the CAP instances, but performs well in the CST instances. On the other hand, when the normalization coefficients are chosen according to MWP, CW or $R\ell_1$ pseudonorms, MIS subproblems perform significantly better. In fact, the best performance in the CST instances is achieved when $R\ell_1$ or CW pseudonorms are used.

In terms of computation time, MWP, CW, $R\ell_1$, and CB yield the best overall computation time in CAP instances, followed by ℓ_1 - and ℓ_∞ -deepest cuts in second place. This is because although deepest cuts are often more effective (particularly ℓ_1 -deepest cuts in the CAP instances), generating these cuts is often computationally more expensive than MWP, CW, $R\ell_1$, and CB, which require solving simpler LPs. Similar observations can be made in CST instances, except ℓ_∞ -deepest cuts along with $R\ell_1$ and CW cuts achieve the best computation times. As expected, since ℓ_2 - and ℓ_4 -deepest cuts require solving relatively large quadratic programs, their computation times do not justify the effectiveness of the cuts. These observations necessitate resorting to a method such as GPA capable of exploiting the structural properties of the problem.

6.4 Numerical Results for the Guided Projections Algorithm

We now present computational results for the BD algorithm when ℓ_p -deepest cuts are generated using the Guided Projections Algorithm 3. Our goal is to assess the effectiveness of GPA in exploiting the combinatorial structure of a problem while producing ℓ_p -deepest cuts for different choices of p . The capacitated facility location problem, which we use in our tests, (29)–(33) exhibits combinatorial structures that can be exploited when solving classical Benders subproblems. Since our intent is to isolate the effect of deepest cuts, we do not employ stabilization techniques in our numerical tests, which would complicate the dynamics and make conclusions harder to draw. A list of such techniques can be found in (Fischetti et al. 2017) and a comprehensive study of their impacts in conjunction with deepest cuts is left to future work.

For a given (fractional) solution \hat{y} , we may derive a Benders cut efficiently by solving the subproblem in the primal space as follows. First, note that constraints (31) can be treated as bounds on the primal variables x . Consequently, it suffices to update these bounds based on values of \hat{y} and reduce the number of constraints in the primal subproblem from $n + k + nk$ to $n + k$ constraints. The resulting problem is a transportation problem, which can be solved efficiently for large instances using specialized algorithms. In our implementation, however, we have used CPLEX for solving the transportation problems since it benefits from better warm starting. Let \hat{u}^D be the optimal dual solution associated with the demand constraints (30) obtained by the solver. Given \hat{u}^D , as noted by several authors (see e.g., Cornuéjols et al. 1991, Fischetti et al. 2016), the Benders cut takes the form

$$\eta \geq \sum_{l=1}^k \hat{u}_l^D + \sum_{j=1}^n \left(f_j + \kappa_j(\hat{u}^D) \right) y_j, \quad (34)$$

where $\kappa_j(\hat{\mathbf{u}}^D)$ is the optimal value of the continuous knapsack problem

$$\kappa_j(\hat{\mathbf{u}}^D) = \min \left\{ \sum_{l=1}^k (d_l c_{lj} - \hat{u}_l^D) \alpha_l : \sum_{l=1}^k \alpha_l d_l \leq s_j, \alpha \in [0, 1]^k \right\},$$

which can be solved efficiently in $\mathcal{O}(k)$ time by finding the weighted median of the ratios $\{c_{lj} - \frac{\hat{u}_l^D}{d_l}\}$ using the procedure given in Balas and Zemel (1980).

Each iteration of GPA (Algorithm 3) for producing an ℓ_p -deepest cut involves finding an ℓ_q -projection (with q such that $1/p + 1/q = 1$), and producing a classical cut using (34). We terminate Algorithm 3 when the ℓ_q -projection $(\hat{\mathbf{y}}^{(h)}, \hat{\boldsymbol{\eta}}^{(h)})$ at iteration h of GPA is sufficiently close to \mathcal{E} as mentioned in Section 5, or after 10 iterations. We considered three choices for ℓ_p -deepest cuts with $p \in \{1, 2, \infty\}$. We also considered the option of switching to classical cuts after the optimality gap falls below a certain threshold (5% in our experiments) to validate the intuitions provided in Section 2.3 which suggest that deepest cuts are more effective at the early iterations of the BD algorithm. Table 2 compares the computational results of six variants of BD equipped with GPA for producing ℓ_p -deepest cuts (with or without switching to classical cuts) with classical Benders (CB) across the CAP and CST benchmark instances. To showcase the benefits of exploiting the structural properties of the problem at a large scale, we have included the large instances of these data sets (i.e. up to 1000 facilities and customers) in Table 2. For brevity, we have excluded the results for smaller instances, but we highlight that GPA is able to reduce the runtime of BD with ℓ_∞ -, ℓ_1 -, and ℓ_2 -deepest cuts by more than 4, 16, and 35 times on average, respectively, compared to the results reported in Table 1 for these norms.

Comparing GPA and CB, we observe that BD equipped with GPA with all choices of $p \in \{1, 2, \infty\}$ has reduced the number of cuts by more than three times on average compared to BD with CB cuts in the large instances of both CAP and CST data sets. The results further confirm effectiveness of deepest cuts in closing the optimality gap, despite the classical cuts in the CFLP (when derived using (34)) often being deemed sufficiently effective in the literature (Fischetti et al. 2016). More importantly, we observe that the running time of BD with GPA is less than half that of BD with CB cuts, even when Euclidean (ℓ_2) deepest cuts are produced. This highlights the effectiveness of GPA in separating the projection and cut generation steps while producing cuts, even when the projection step requires solving a quadratic program. Finally, we observe that employing deepest cuts at the early iterations of the BD algorithm and switching to classical cuts after a certain threshold (5% optimality gap in our tests) has a positive effect on the overall number of cuts produced and on the computation time, which supports the theoretical insights provided in Section 2.3.

7 Conclusions

In this paper, we proposed and analyzed theoretically and computationally a new method for selecting Benders cuts, aimed at improving the effectiveness of the cuts in closing the gap and reducing the running time of the BD algorithm. Our technique is based on generating Benders cuts that explicitly take cut depth into account. As a measure of cut depth, we considered Euclidean distance from the master solution to the candidate cuts, and then extended this measure to general ℓ_p -norms. We provided a comprehensive study of deepest cuts and unveiled their properties from a primal perspective. We showed that producing an ℓ_p -deepest cut is equivalent to finding an ℓ_q -projection of the point being separated onto the epigraph of the original problem. We also showed how the separation problems can be solved as linear or quadratic programs. Leveraging the duality between ℓ_p -deepest cuts and ℓ_q -projections, we introduced our Guided Projections Algorithm for producing ℓ_p -deepest cuts in a way that can exploit the combinatorial structure of problem instances.

Instance	Cuts							Time (sec.)						
	CB	Without switch			Switch at 5%			CB	Without switch			Switch at 5%		
		ℓ_1	ℓ_∞	ℓ_2	ℓ_1	ℓ_∞	ℓ_2		ℓ_1	ℓ_∞	ℓ_2	ℓ_1	ℓ_∞	ℓ_2
CAPa* (100,1000)	105.8	48.8	62.3	46.8	41.5	51.0	44.8	18.66	16.32	15.98	13.98	11.40	14.59	13.39
CAPb* (100,1000)	413.3	155.8	104.5	95.0	115.8	106.8	101.0	52.42	35.72	18.13	19.75	24.90	17.91	21.21
CAPc* (100,1000)	320.8	127.3	97.0	91.8	107.5	92.0	81.5	37.65	27.57	14.90	15.84	19.14	14.36	14.50
Mean	280.0	110.6	87.9	77.8	88.3	83.3	75.8	36.24	26.54	16.33	16.52	18.48	15.62	16.36
CST (100,500,5)	59.0	34.3	20.8	9.5	19.3	13.0	13.8	3.57	2.23	1.31	1.01	1.68	1.10	1.29
CST (100,500,10)	68.5	54.3	36.5	38.8	27.8	30.3	32.0	4.51	3.48	2.67	3.46	2.29	2.53	3.01
CST (100,500,15)	87.5	62.8	29.8	54.5	36.3	19.8	22.8	6.29	4.13	2.65	4.91	2.90	2.11	2.57
CST (100,500,20)	65.3	56.3	40.3	32.0	29.3	23.5	30.8	5.32	4.35	3.12	3.29	2.68	2.51	3.26
CST (500,500,5)	28.8	8.5	8.5	8.8	6.0	5.5	6.8	9.30	4.77	4.53	4.82	4.46	4.08	4.68
CST (500,500,10)	69.3	57.5	63.3	66.0	42.0	28.0	53.8	23.72	19.44	17.60	24.12	15.98	12.57	22.17
CST (500,500,15)	75.7	30.5	38.8	27.3	46.8	7.0	46.3	26.03	14.85	14.89	15.03	20.45	7.46	22.53
CST (500,500,20)	127.5	53.5	40.3	43.3	10.3	27.8	8.8	50.84	23.12	18.67	23.20	9.55	15.57	11.39
CST (100,1000,5)	88.5	36.0	24.3	42.5	26.0	22.0	31.3	11.62	5.23	4.07	6.58	4.49	3.74	5.62
CST (100,1000,10)	125.3	83.3	57.3	48.3	34.0	43.3	44.3	19.40	12.24	10.53	9.67	7.15	9.29	10.14
CST (100,1000,15)	81.8	65.3	66.8	65.5	52.8	60.0	54.8	16.59	12.82	13.54	14.69	11.13	13.02	12.49
CST (100,1000,20)	78.5	64.3	54.0	56.8	47.0	49.8	42.5	19.93	15.67	13.32	13.99	11.39	13.38	12.28
Mean	79.6	50.5	40.0	41.1	31.4	27.5	32.3	16.43	10.20	8.91	10.40	7.84	7.28	9.29
CST (200,1000,5)	56.8	8.3	9.8	9.5	7.8	5.3	5.5	14.44	4.44	4.72	4.78	4.49	3.82	3.79
CST (200,1000,10)	180.3	31.8	41.5	62.0	21.8	37.5	32.8	59.96	14.25	17.86	22.84	12.46	17.94	16.23
CST (200,1000,15)	204.5	83.8	84.3	78.5	52.3	50.3	65.0	70.66	29.23	32.55	34.69	26.40	26.96	33.84
CST (200,1000,20)	170.5	127.3	78.8	76.8	60.8	72.0	105.8	73.83	44.09	35.18	37.34	34.05	39.03	51.87
CST (500,1000,5)	29.3	34.0	14.5	18.0	21.3	4.5	22.3	22.71	25.58	14.98	18.16	20.53	10.30	20.66
CST (500,1000,10)	131.5	37.0	43.3	45.3	40.3	22.0	31.3	122.92	37.28	37.71	45.95	42.04	31.75	38.27
CST (500,1000,15)	127.5	31.5	40.5	18.8	23.3	22.0	26.3	133.71	42.07	48.58	36.23	38.34	39.83	46.70
CST (500,1000,20)	252.0	27.3	69.5	115.8	20.5	39.3	41.8	389.08	48.79	94.76	143.77	45.71	74.17	85.31
CST (1000,1000,5)	3.5	2.0	2.0	2.0	2.0	2.0	2.0	22.82	15.66	15.48	16.07	15.43	14.92	15.27
CST (1000,1000,10)	46.5	5.0	5.0	4.5	4.0	3.0	3.5	97.55	31.17	29.99	27.61	29.53	24.99	25.98
CST (1000,1000,15)	204.3	59.5	67.8	88.8	48.3	27.0	65.5	684.32	171.47	155.73	214.40	144.51	104.71	193.88
CST (1000,1000,20)	103.0	12.3	8.0	9.8	10.0	6.3	7.0	280.88	79.79	78.10	81.37	74.48	77.29	80.41
Mean	125.8	38.3	38.7	44.1	26.0	24.3	34.0	164.41	45.32	47.14	56.94	40.66	38.81	51.01

Table 2: Computational performance of BD algorithm using GPA for producing deepest cuts on large instances of CAT and CST data sets, where cuts are generated by exploiting the combinatorial structures of the instances.

From a theoretical perspective, we generalized our notion of distance by defining what we call a Benders distance function, and developed a notion of monotonicity which allows these functions to be treated as distance functions despite the fact that they do not necessarily satisfy the axioms of metrics. Then, we illustrated the connection of such distance functions to some well-known cut selection strategies. Specifically, we established the connection to MIS cuts, and provided three novel ways of choosing the normalization coefficients in the MIS subproblem, that connect our distance functions to the Magnanti-Wong procedure for producing Pareto-optimal cuts, as well as the Conforti-Wolsey procedure for producing facet-defining cuts.

Our computational experiments on CFLP instances showed the benefits of deepest cuts and other distance-based cuts, particularly when generated using GPA, in decreasing the number of cuts as well as the runtime of the BD algorithm. Besides the theoretical insights, our results showed that deepest cuts are effective in speeding up convergence of BD. Our results also illustrated the benefits of choosing specific normalization coefficients in the MIS problems based on parameters of the problem instances.

References

- Adulyasak Y, Cordeau JF, Jans R (2015) Benders Decomposition for production routing under demand uncertainty. *Operations Research* 63(4):851–867.
- Alshamsi A, Diabat A (2018) Large-scale reverse supply chain network design: An accelerated Benders Decomposition algorithm. *Computers & Industrial Engineering* 124:545–559.
- Balas E, Ceria S, Cornuéjols G (1993) A lift-and-project cutting plane algorithm for mixed 0–1 programs. *Mathematical Programming* 58(1-3):295–324.
- Balas E, Zemel E (1980) An algorithm for large zero-one knapsack problems. *Operations Research* 28(5):1130–1154.
- Bayram V, Yaman H (2017) Shelter location and evacuation route assignment under uncertainty: A Benders Decomposition approach. *Transportation Science* 52(2):416–436.
- Beasley J (2021) ORLIB. <http://people.brunel.ac.uk/~mastjjb/jeb/orlib/capinfo.html>.
- Benders JF (1962) Partitioning procedures for solving mixed-variables programming problems. *Numerische Mathematik* 4(1):238–252.
- Bodur M, Dash S, Günlük O, Luedtke J (2016) Strengthened Benders cuts for stochastic integer programs with continuous recourse. *INFORMS Journal on Computing* 29(1):77–91.
- Bodur M, Luedtke JR (2016) Mixed-integer rounding enhanced Benders Decomposition for multiclass service-system staffing and scheduling with arrival rate uncertainty. *Management Science* 63(7):2073–2091.
- Bonami P, Salvagnin D, Tramontani A (2020) Implementing automatic Benders Decomposition in a modern MIP solver. *International Conference on Integer Programming and Combinatorial Optimization*, 78–90 (Springer).
- Cadoux F (2010) Computing deep facet-defining disjunctive cuts for mixed-integer programming. *Mathematical Programming* 122(2):197–223.
- Charnes A, Cooper WW (1962) Programming with linear fractional functionals. *Naval Research Logistics Quarterly* 9(3-4):181–186.
- Cho SH, Jang H, Lee T, Turner J (2014) Simultaneous location of trauma centers and helicopters for emergency medical service planning. *Operations Research* 62(4):751–771.
- Codato G, Fischetti M (2006) Combinatorial Benders’ cuts for mixed-integer linear programming. *Operations Research* 54(4):756–766.
- Conforti M, Wolsey LA (2019) “facet” separation with one linear program. *Mathematical Programming* 178(1):361–380.
- Contreras I, Cordeau JF, Laporte G (2011) Benders Decomposition for large-scale uncapacitated hub location. *Operations Research* 59(6):1477–1490.
- Contreras I, Cordeau JF, Laporte G (2012) Exact solution of large-scale hub location problems with multiple capacity levels. *Transportation Science* 46(4):439–459.
- Cornuéjols G, Sridharan R, Thizy JM (1991) A comparison of heuristics and relaxations for the capacitated plant location problem. *European Journal of Operational Research* 50(3):280–297.
- de Sá EM, de Camargo RS, de Miranda G (2013) An improved Benders Decomposition algorithm for the tree of hubs location problem. *European Journal of Operational Research* 226(2):185–202.
- Drezner Z, Hamacher HW (2001) *Facility location: applications and theory* (Springer Science & Business Media).
- Fischetti M, Ljubić I, Sinnl M (2016) Benders Decomposition without separability: A computational study for capacitated facility location problems. *European Journal of Operational Research* 253(3):557–569.
- Fischetti M, Ljubić I, Sinnl M (2017) Redesigning Benders Decomposition for large-scale facility location. *Management Science* 63(7):2146–2162.
- Fischetti M, Salvagnin D, Zanette A (2010) A note on the selection of Benders cuts. *Mathematical Programming* 124(1-2):175–182.
- Fontaine P, Minner S (2018) Benders Decomposition for the hazmat transport network design problem. *European Journal of Operational Research* 267(3):996–1002.
- Fortz B, Poss M (2009) An improved benders decomposition applied to a multi-layer network design problem. *Operations Research Letters* 37(5):359–364.
- Geoffrion AM (1972) Generalized Benders Decomposition. *Journal of Optimization Theory and Applications* 10(4):237–260.

- Hooker JN, Ottosson G (2003) Logic-based Benders Decomposition. *Mathematical Programming* 96(1):33–60.
- Keyvanshokoo E, Ryan SM, Kabir E (2016) Hybrid robust and stochastic optimization for closed-loop supply chain network design using accelerated Benders Decomposition. *European Journal of Operational Research* 249(1):76–92.
- Khassiba A, Bastin F, Cafieri S, Gendron B, Mongeau M (2020) Two-stage stochastic mixed-integer programming with chance constraints for extended aircraft arrival management. *Transportation Science* 54(4):897–919.
- Magnanti TL, Wong RT (1981) Accelerating Benders Decomposition: Algorithmic enhancement and model selection criteria. *Operations Research* 29(3):464–484.
- Maheo A, Kilby P, Van Hentenryck P (2017) Benders Decomposition for the design of a hub and shuttle public transit system. *Transportation Science* 53(1):77–88.
- Mercier A (2008) A theoretical comparison of feasibility cuts for the integrated aircraft-routing and crew-pairing problem. *Transportation Science* 42(1):87–104.
- Naderi B, Roshanaei V, Begen MA, Aleman DM, Urbach DR (2021) Increased surgical capacity without additional resources: Generalized operating room planning and scheduling. *Production and Operations Management* .
- Papadacos N (2008) Practical enhancements to the Magnanti–Wong method. *Operations Research Letters* 36(4):444–449.
- Papadacos N (2009) Integrated airline scheduling. *Computers & Operations Research* 36(1):176–195.
- Pearce RH, Forbes M (2018) Disaggregated Benders Decomposition and branch-and-cut for solving the budget-constrained dynamic uncapacitated facility location and network design problem. *European Journal of Operational Research* 270(1):78–88.
- Rahimi A, Gönen M (2021) Efficient multitask multiple kernel learning with application to cancer research. *IEEE Transactions on Cybernetics* 1–13, URL <http://dx.doi.org/10.1109/TCYB.2021.3052357>.
- Rahmaniani R, Crainic TG, Gendreau M, Rei W (2017) The Benders Decomposition algorithm: A literature review. *European Journal of Operational Research* 259(3):801–817.
- Rahmaniani R, Crainic TG, Gendreau M, Rei W (2018) Accelerating the Benders Decomposition method: Application to stochastic network design problems. *SIAM Journal on Optimization* 28(1):875–903.
- Saharidis GK, Ierapetritou MG (2010) Improving Benders Decomposition using maximum feasible subsystem (MFS) cut generation strategy. *Computers & Chemical Engineering* 34(8):1237–1245.
- Santoso T, Ahmed S, Goetschalckx M, Shapiro A (2005) A stochastic programming approach for supply chain network design under uncertainty. *European Journal of Operational Research* 167(1):96–115.
- Sherali HD, Lunday BJ (2013) On generating maximal nondominated Benders cuts. *Annals of Operations Research* 210(1):57–72.
- Taherkhani G, Alumur SA, Hosseini M (2020) Benders Decomposition for the profit maximizing capacitated hub location problem with multiple demand classes. *Transportation Science* 54(6):1446–1470.
- Taherkhani G, Alumur SA, Hosseini M (2021) Robust-stochastic models for profit maximizing hub location problems. *Transportation Science* .
- Tibshirani R (1996) Regression shrinkage and selection via the lasso. *Journal of the Royal Statistical Society: Series B (Methodological)* 58(1):267–288.

A Proof of Theorems

In this appendix, we provide the proof of the propositions and theorems given in the body of the paper. For convenience, we formally restate the propositions and theorems as well.

Proposition 1. *Solution (\mathbf{y}, η) satisfies constraints (14) if and only if $(\mathbf{y}, \eta) \in \mathcal{E}$.*

Proof. We first show that any $(\mathbf{y}, \eta) \in \mathcal{E}$ satisfies all constraints (14). It suffices to show that constraints (14) are implied by the classical Benders cuts. For an arbitrary certificate $(\boldsymbol{\pi}, \pi_0)$, we may consider two cases:

Case 1: For $\pi_0 > 0$, define $\mathbf{u} = \frac{\boldsymbol{\pi}}{\pi_0}$. Then, $\mathbf{u} \geq \mathbf{0}$ and $\mathbf{u}^\top A \leq \mathbf{c}^\top$, implying $\mathbf{u} \in \mathcal{U}$. Consequently, by Minkowski's representation theorem, \mathbf{u} is a convex combination of extreme points of \mathcal{U} and a weighted combination of extreme rays of \mathcal{U} , which implies that constraint $0 \geq \boldsymbol{\pi}^\top (\mathbf{b} - B\mathbf{y}) + \pi_0(\mathbf{f}^\top \mathbf{y} - \eta)$ is implied by the classical Benders feasibility and optimality cuts.

Case 2: For $\pi_0 = 0$, we have $\boldsymbol{\pi}^\top A \leq \mathbf{0}$, which means $\boldsymbol{\pi}$ is in the recession cone of \mathcal{U} . Consequently, constraint $0 \geq \boldsymbol{\pi}^\top (\mathbf{b} - B\mathbf{y}) + \pi_0(\mathbf{f}^\top \mathbf{y} - \eta) = \boldsymbol{\pi}^\top (\mathbf{b} - B\mathbf{y})$ is implied by the classical Benders feasibility cuts.

Next, we show that any (\mathbf{y}, η) satisfying constraints (14) belongs to \mathcal{E} . Observe that any extreme point \mathbf{u} of \mathcal{U} can be represented as a certificate $(\boldsymbol{\pi}, \pi_0) = (\mathbf{u}, 1)$. Similarly, any extreme ray \mathbf{v} of \mathcal{U} can be represented as a certificate $(\boldsymbol{\pi}, \pi_0) = (\mathbf{v}, 0)$. Consequently, constraint set (14) contains all classical Benders optimality and feasibility cuts. \square

Proposition 2. *Given $q \geq 1$ and $\hat{\mathbf{z}} \in \mathbb{R}^{n+1}$, the minimum ℓ_q -distance from the point $\hat{\mathbf{z}}$ to the points on the hyperplane $\boldsymbol{\alpha}^\top \mathbf{z} + \beta = 0$ is*

$$\min_{\mathbf{z}: \boldsymbol{\alpha}^\top \mathbf{z} + \beta = 0} \|\mathbf{z} - \hat{\mathbf{z}}\|_q = \frac{|\boldsymbol{\alpha}^\top \hat{\mathbf{z}} + \beta|}{\|\boldsymbol{\alpha}\|_p},$$

where ℓ_p is the dual norm of ℓ_q (i.e., $\frac{1}{p} + \frac{1}{q} = 1$).

Proof. For generality, we prove the proposition for general norms using the definition of dual norms; proof for ℓ_p norms follows directly. By definition of dual norms, we have

$$\|\boldsymbol{\alpha}\|_* = \max_x \left\{ \frac{|\boldsymbol{\alpha}^\top \mathbf{x}|}{\|\mathbf{x}\|} \right\}.$$

Replacing $\mathbf{x} = \mathbf{z} - \hat{\mathbf{z}}$, we get

$$\|\boldsymbol{\alpha}\|_* = \max_z \left\{ \frac{|\boldsymbol{\alpha}^\top (\mathbf{z} - \hat{\mathbf{z}})|}{\|\mathbf{z} - \hat{\mathbf{z}}\|} \right\}. \quad (35)$$

For $\mathbf{z} \in \mathbb{R}^{n+1} \setminus \{\hat{\mathbf{z}}\}$, define $\tilde{\mathbf{z}}(\mathbf{z})$ to be the intersection of hyperplane $\boldsymbol{\alpha}^\top \mathbf{z} + \beta = 0$ and the line that crosses points $(\mathbf{z}, \hat{\mathbf{z}})$. Note that the intersection point for any optimal \mathbf{z} exists, since the line crossing $(\mathbf{z}, \hat{\mathbf{z}})$ cannot be parallel to the hyperplane $\boldsymbol{\alpha}^\top \mathbf{z} + \beta = 0$ for optimal \mathbf{z} . This is because a parallel line crossing $(\mathbf{z}, \hat{\mathbf{z}})$ and hyperplane $\boldsymbol{\alpha}^\top \mathbf{z} + \beta = 0$ would imply that $\boldsymbol{\alpha}^\top (\mathbf{z} - \hat{\mathbf{z}}) = 0$, which cannot be optimal, since $\|\boldsymbol{\alpha}\|_* > 0$. Now, since $\hat{\mathbf{z}}$ does not belong to the hyperplane $\boldsymbol{\alpha}^\top \mathbf{z} + \beta = 0$, there exists $\theta(\mathbf{z}) \neq 0$ such that $\mathbf{z} - \hat{\mathbf{z}} = \theta(\mathbf{z}) \times (\tilde{\mathbf{z}}(\mathbf{z}) - \hat{\mathbf{z}})$. We can therefore rewrite (35) as

$$\|\boldsymbol{\alpha}\|_* = \max_z \left\{ \frac{|\theta(\mathbf{z})| |\boldsymbol{\alpha}^\top (\tilde{\mathbf{z}}(\mathbf{z}) - \hat{\mathbf{z}})|}{\|\theta(\mathbf{z}) \times (\tilde{\mathbf{z}}(\mathbf{z}) - \hat{\mathbf{z}})\|} \right\} = \max_z \left\{ \frac{|\boldsymbol{\alpha}^\top (\tilde{\mathbf{z}}(\mathbf{z}) - \hat{\mathbf{z}})|}{\|(\tilde{\mathbf{z}}(\mathbf{z}) - \hat{\mathbf{z}})\|} \right\}, \quad (36)$$

where the last equality holds since norms are homogeneous. Consequently, without loss of generality we may restrict z to the points on the hyperplane $\alpha^\top z + \beta = 0$, that is

$$\|\alpha\|_* = \max_{z: \alpha^\top z + \beta = 0} \left\{ \frac{|\alpha^\top (z - \hat{z})|}{\|z - \hat{z}\|} \right\} = \max_{z: \alpha^\top z + \beta = 0} \left\{ \frac{|\alpha^\top \hat{z} + \beta|}{\|z - \hat{z}\|} \right\}, \quad (37)$$

where we have used $\beta = -\alpha^\top \hat{z}$. But $|\alpha^\top \hat{z} + \beta|$ is constant, therefore we may rewrite (37) as

$$\|\alpha\|_* = |\alpha^\top \hat{z} + \beta| \max_{z: \alpha^\top z + \beta = 0} \left\{ \frac{1}{\|z - \hat{z}\|} \right\} = \frac{|\alpha^\top \hat{z} + \beta|}{\min_{z: \alpha^\top z + \beta = 0} \|z - \hat{z}\|}, \quad (38)$$

which completes the proof for general norm. The proof for ℓ_q follows by replacing $\|\cdot\| = \|\cdot\|_q$ and $\|\cdot\|_* = \|\cdot\|_p$. \square

Theorem 1. Separation problem (18) is equivalent to the following Lagrangian dual problem.

$$\begin{aligned} [\text{Primal SSP}] \quad & \min \quad \|(\mathbf{y} - \hat{\mathbf{y}}, \eta - \hat{\eta})\|_q \\ & \text{s.t.} \quad \eta \geq \mathbf{c}^\top \mathbf{x} + \mathbf{f}^\top \mathbf{y} \\ & \quad \quad \quad \mathbf{A}\mathbf{x} \geq \mathbf{b} - \mathbf{B}\mathbf{y} \\ & \quad \quad \quad \mathbf{x} \geq \mathbf{0}, \end{aligned} \quad (39)$$

in which $(\mathbf{y}, \mathbf{x}, \eta)$ are the variables and ℓ_q is the dual norm of ℓ_p .

Proof. SSP (18) can be equivalently stated as (see Proposition 9):

$$\begin{aligned} & \max_{(\boldsymbol{\pi}, \pi_0) \in \Pi} \quad \boldsymbol{\pi}^\top (\mathbf{b} - \mathbf{B}\hat{\mathbf{y}}) + \pi_0 (\mathbf{f}^\top \hat{\mathbf{y}} - \hat{\eta}) \\ & \text{s.t.} \quad \|(\pi_0 \mathbf{f}^\top - \boldsymbol{\pi}^\top \mathbf{B}, \pi_0)\|_p \leq 1. \end{aligned} \quad (40)$$

In the following, we prove the statement for $p < \infty$, since for $p = \infty$ the dual can be directly derived using LP duality by reformulating (40) as an LP (see Section 4.1). For $p < \infty$, $\|(\pi_0 \mathbf{f}^\top - \boldsymbol{\pi}^\top \mathbf{B}, \pi_0)\|_p \leq 1$ is equivalent to $\pi_0^p + \sum_{j=1}^n |\pi_0 f_j - \boldsymbol{\pi}^\top B_j|^p \leq 1$, where B_j is the j 'th column of matrix B . Hence, introducing non-negative variables τ_j , $j = 1, \dots, n$, we may restate (40) as

$$\max \quad \boldsymbol{\pi}^\top (\mathbf{b} - \mathbf{B}\hat{\mathbf{y}}) + \pi_0 (\mathbf{f}^\top \hat{\mathbf{y}} - \hat{\eta}) \quad (41)$$

$$\text{s.t.} \quad \boldsymbol{\pi}^\top \mathbf{A} - \pi_0 \mathbf{c}^\top \leq \mathbf{0} \quad (42)$$

$$\pi_0^p + \sum_{j=1}^n \tau_j^p \leq 1 \quad (43)$$

$$\pi_0 \mathbf{f}^\top - \boldsymbol{\pi}^\top \mathbf{B} \leq \boldsymbol{\tau}^\top \quad (44)$$

$$\boldsymbol{\pi}^\top \mathbf{B} - \pi_0 \mathbf{f}^\top \leq \boldsymbol{\tau}^\top \quad (45)$$

$$\boldsymbol{\pi} \geq \mathbf{0}, \boldsymbol{\tau} \geq \mathbf{0}, \pi_0 \geq 0. \quad (46)$$

Assigning Lagrange multipliers \mathbf{x} , δ_0 , \mathbf{y}^- and \mathbf{y}^+ respectively to constraints (42)-(45), we can derive the following Lagrangian dual problem

$$\min \quad \|(\mathbf{y}^+ + \mathbf{y}^-, \delta_0)\|_q \quad (47)$$

$$\text{s.t.} \quad \mathbf{c}^\top \mathbf{x} \leq \hat{\eta} + \delta_0 - \mathbf{f}^\top (\hat{\mathbf{y}} + \mathbf{y}^+ - \mathbf{y}^-) \quad (48)$$

$$\mathbf{A}\mathbf{x} \geq \mathbf{b} - \mathbf{B}(\hat{\mathbf{y}} + \mathbf{y}^+ - \mathbf{y}^-) \quad (49)$$

$$\mathbf{x} \geq \mathbf{0}, \delta_0 \geq 0, \mathbf{y}^+ \geq \mathbf{0}, \mathbf{y}^- \geq \mathbf{0}. \quad (50)$$

The dual problem (39) is derived by replacing $\mathbf{y} = \hat{\mathbf{y}} + \mathbf{y}^+ - \mathbf{y}^-$ and noting that minimizing $y_j^+ + y_j^-$ is equivalent to minimizing $|y_j - \hat{y}_j|$. Finally, as we will show in Proposition 9, constraint (43) is binding at optimality; thus, at optimality $\delta_0 \geq 0$ and we may suppress this constraint. \square

Proposition 3. *Let $(\tilde{\mathbf{y}}, \tilde{\eta}) \in \mathcal{E}$ be an ℓ_q -projection of $(\hat{\mathbf{y}}, \hat{\eta})$ onto \mathcal{E} . Then, any ℓ_p -deepest cut separating $(\hat{\mathbf{y}}, \hat{\eta})$ from \mathcal{E} supports \mathcal{E} at $(\tilde{\mathbf{y}}, \tilde{\eta})$.*

Proof. Let $(\hat{\boldsymbol{\pi}}, \hat{\pi}_0)$ be the solution associated with the ℓ_p -deepest cut. By Theorem 1 we have

$$\|(\tilde{\mathbf{y}} - \hat{\mathbf{y}}, \tilde{\eta} - \hat{\eta})\|_q = \frac{\hat{\boldsymbol{\pi}}^\top (\mathbf{b} - B\hat{\mathbf{y}}) + \hat{\pi}_0 (\mathbf{f}^\top \hat{\mathbf{y}} - \hat{\eta})}{\|(\hat{\boldsymbol{\pi}}^\top B - \hat{\pi}_0 \mathbf{f}^\top, \hat{\pi}_0)\|_p}. \quad (51)$$

On the other hand, $(\tilde{\mathbf{y}}, \tilde{\eta}) \in \mathcal{E}$ implies $\hat{\boldsymbol{\pi}}^\top (\mathbf{b} - B\tilde{\mathbf{y}}) + \hat{\pi}_0 (\mathbf{f}^\top \tilde{\mathbf{y}} - \tilde{\eta}) \leq 0$. To the contrary, assume that $(\tilde{\mathbf{y}}, \tilde{\eta})$ is not on the hyperplane. Then, $\hat{\boldsymbol{\pi}}^\top (\mathbf{b} - B\tilde{\mathbf{y}}) + \hat{\pi}_0 (\mathbf{f}^\top \tilde{\mathbf{y}} - \tilde{\eta})$ must be negative, implying

$$0 < -\frac{\hat{\boldsymbol{\pi}}^\top (\mathbf{b} - B\tilde{\mathbf{y}}) + \hat{\pi}_0 (\mathbf{f}^\top \tilde{\mathbf{y}} - \tilde{\eta})}{\|(\hat{\boldsymbol{\pi}}^\top B - \hat{\pi}_0 \mathbf{f}^\top, \hat{\pi}_0)\|_p}. \quad (52)$$

Adding (51) and (52) we get

$$\|(\tilde{\mathbf{y}} - \hat{\mathbf{y}}, \tilde{\eta} - \hat{\eta})\|_q < \frac{(\hat{\boldsymbol{\pi}}^\top B - \hat{\pi}_0 \mathbf{f}^\top)(\tilde{\mathbf{y}} - \hat{\mathbf{y}}) + \hat{\pi}_0(\tilde{\eta} - \hat{\eta})}{\|(\hat{\boldsymbol{\pi}}^\top B - \hat{\pi}_0 \mathbf{f}^\top, \hat{\pi}_0)\|_p}.$$

But this contradicts with Hölder's inequality since ℓ_p and ℓ_q are dual norms. \square

Proposition 4. *For sufficiently small $\hat{\eta}$, the ℓ_1 -deepest cut separating $(\hat{\mathbf{y}}, \hat{\eta})$ from \mathcal{E} is the flat cut $\eta \geq Q^*$, where $Q^* = \min_{\mathbf{y}} Q(\mathbf{y})$ is the optimal value of Q for unrestricted \mathbf{y} .*

Proof. Since the dual norm of ℓ_1 is ℓ_∞ , the objective function in Primal SSP (19) is to minimize the component with largest absolute value in $(\mathbf{y} - \hat{\mathbf{y}}, \eta - \hat{\eta})$, which, for sufficiently small $\hat{\eta}$, is $|\eta - \hat{\eta}| = \eta - \hat{\eta}$. Thus, we can restate Primal SSP as the following LP

$$\begin{aligned} & -\hat{\eta} + \min \quad \eta \\ & \text{s.t.} \quad \eta \geq \mathbf{c}^\top \mathbf{x} + \mathbf{f}^\top \mathbf{y} \\ & \quad \quad \quad A\mathbf{x} \geq \mathbf{b} - B\mathbf{y} \\ & \quad \quad \quad \mathbf{x} \geq \mathbf{0}. \end{aligned} \quad (53)$$

Let $(\hat{\eta}, \hat{\mathbf{y}}, \hat{\mathbf{x}})$ be the optimal solution of (53). Observe that $\hat{\eta} = Q(\hat{\mathbf{y}}) = \min_{\mathbf{y}} Q(\mathbf{y})$, that is $(\hat{\eta}, \hat{\mathbf{y}})$ is an optimal corner point of \mathcal{E} . Further, let π_0 and $\boldsymbol{\pi}$ be the dual multipliers. The dual LP reads as

$$\begin{aligned} & -\hat{\eta} + \max \quad \boldsymbol{\pi}^\top \mathbf{b} \\ & \text{s.t.} \quad \boldsymbol{\pi}^\top A \leq \pi_0 \mathbf{c} \\ & \quad \quad \quad \boldsymbol{\pi}^\top B = \pi_0 \mathbf{f} \\ & \quad \quad \quad \pi_0 = 1 \\ & \quad \quad \quad \boldsymbol{\pi} \geq \mathbf{0}. \end{aligned} \quad (54)$$

Let $(\hat{\boldsymbol{\pi}}, \hat{\pi}_0)$ be the optimal solution to (54). The ℓ_1 -deepest cut is $\hat{\boldsymbol{\pi}}^\top (\mathbf{b} - B\mathbf{y}) + \hat{\pi}_0 (\mathbf{f}^\top \mathbf{y} - \eta) = \hat{\boldsymbol{\pi}}^\top \mathbf{b} - \eta \leq 0$. By strong duality, $\hat{\boldsymbol{\pi}}^\top \mathbf{b} = \hat{\eta} = Q^*$, hence the deepest cut is the flat cut $\eta \geq Q^*$. \square

Proposition 5. Let $Q^* = \min_{\mathbf{y}} Q(\mathbf{y})$ be the optimal unrestricted value of Q . Provided that $\hat{\eta} < Q^*$ and $p > 1$, the ℓ_p -deepest cut that separates $(\hat{\mathbf{y}}, \hat{\eta})$ is an optimality cut for any arbitrary $\hat{\mathbf{y}}$ (i.e., even if $\hat{\mathbf{y}} \notin \text{dom}(Q)$).

Proof. Since $\hat{\eta} < Q^*$, we can separate $(\hat{\mathbf{y}}, \hat{\eta})$ from \mathcal{E} using the flat cut $\bar{\mathcal{H}} = \{(\mathbf{y}, \eta) : \eta \geq Q^*\}$. Let $(\hat{\boldsymbol{\pi}}, \hat{\pi}_0) \in \Pi$ be the dual solution associated with the deepest cut, and assume to the contrary that the deepest cut is vertical, that is $\hat{\pi}_0 = 0$.

Let $(\tilde{\mathbf{y}}^H, \tilde{\eta}^H)$ and $(\tilde{\mathbf{y}}^V, \tilde{\eta}^V)$ be the ℓ_q -projections of $(\hat{\mathbf{y}}, \hat{\eta})$ onto $\bar{\mathcal{H}}$ and $\mathcal{H}(\hat{\boldsymbol{\pi}}, \hat{\pi}_0)$, respectively. Observe that $(\tilde{\mathbf{y}}^H, \tilde{\eta}^H) = (\hat{\mathbf{y}}, Q^*)$ and $\tilde{\eta}^V = \hat{\eta}$, and that the ℓ_q -projection of $(\hat{\mathbf{y}}, \hat{\eta})$ onto $\bar{\mathcal{H}} \cap \mathcal{H}(\hat{\boldsymbol{\pi}}, \hat{\pi}_0)$ is $(\tilde{\mathbf{y}}^V, \tilde{\eta}^H)$. Let \bar{d} be the ℓ_q -distance of $(\hat{\mathbf{y}}, \hat{\eta})$ from $\bar{\mathcal{H}} \cap \mathcal{H}(\hat{\boldsymbol{\pi}}, \hat{\pi}_0)$. Note that

$$\begin{aligned} \bar{d} &= \|(\hat{\mathbf{y}}, \hat{\eta}) - (\tilde{\mathbf{y}}^V, \tilde{\eta}^H)\|_q = \left(\|\hat{\mathbf{y}} - \tilde{\mathbf{y}}^V\|_q^q + \|\hat{\eta} - \tilde{\eta}^H\|_q^q \right)^{\frac{1}{q}} \\ &= \left(\|\hat{\mathbf{y}} - \tilde{\mathbf{y}}^V\|_q^q + \|\hat{\eta} - \tilde{\eta}^V\|_q^q + \|\hat{\mathbf{y}} - \tilde{\mathbf{y}}^H\|_q^q + \|\hat{\eta} - \tilde{\eta}^H\|_q^q \right)^{\frac{1}{q}} \\ &= \left(\|(\hat{\mathbf{y}}, \hat{\eta}) - (\tilde{\mathbf{y}}^V, \tilde{\eta}^V)\|_q^q + \|(\hat{\mathbf{y}}, \hat{\eta}) - (\tilde{\mathbf{y}}^H, \tilde{\eta}^H)\|_q^q \right)^{\frac{1}{q}} \\ &= ((d^*)^q + (Q^* - \hat{\eta})^q)^{\frac{1}{q}}, \end{aligned}$$

where $d^* = \|(\hat{\mathbf{y}}, \hat{\eta}) - (\tilde{\mathbf{y}}^V, \tilde{\eta}^V)\|_q$. This implies that $\bar{d} > d^*$ since $q < \infty$ and $Q^* > \hat{\eta}$. However, both $\bar{\mathcal{H}}$ and $\mathcal{H}(\hat{\boldsymbol{\pi}}, \hat{\pi}_0)$ support \mathcal{E} , therefore ℓ_q -distance of $(\hat{\mathbf{y}}, \hat{\eta})$ from \mathcal{E} (i.e., d^*) must be at least equal to \bar{d} , that is $d^* \geq \bar{d}$, which is a contradiction. \square

Proposition 6. Let $(\tilde{\mathbf{y}}, \tilde{\eta})$ be the unique ℓ_q -projection of $(\hat{\mathbf{y}}, \hat{\eta})$ onto \mathcal{E} . If $\hat{\eta} < \tilde{\eta}$, then the ℓ_p -deepest cuts separating $(\hat{\mathbf{y}}, \hat{\eta})$ are optimality cuts for any arbitrary $\hat{\mathbf{y}}$ (i.e., even if $\hat{\mathbf{y}} \notin \text{dom}(Q)$).

Proof. Let $(\hat{\boldsymbol{\pi}}, \hat{\pi}_0) \in \Pi$ be the dual solution associated with the deepest cut. Assume to the contrary that the deepest cut is a feasibility cut, that is $\hat{\pi}_0 = 0$. Since the projection is unique, the ℓ_q -projection of $(\hat{\mathbf{y}}, \hat{\eta})$ onto the vertical cut $\mathcal{H}(\hat{\boldsymbol{\pi}}, \hat{\pi}_0)$ must be $(\tilde{\mathbf{y}}, \hat{\eta})$, which contradicts with the assumption that $\tilde{\eta} > \hat{\eta}$. \square

Proposition 7. Epigraph distance function d^* certifies $d^*(\hat{\mathbf{y}}, \hat{\eta}) > 0$ iff $(\hat{\mathbf{y}}, \hat{\eta})$ is in the exterior of \mathcal{E} , $d^*(\hat{\mathbf{y}}, \hat{\eta}) = 0$ iff $(\hat{\mathbf{y}}, \hat{\eta})$ is on the boundary of \mathcal{E} , and $d^*(\hat{\mathbf{y}}, \hat{\eta}) < 0$ iff $(\hat{\mathbf{y}}, \hat{\eta})$ is in the interior of \mathcal{E} .

Proof. The proof follows from definition of d^* and noting that \mathcal{E} is the intersection of half-spaces $\mathcal{H}(\boldsymbol{\pi}, \pi_0)$ for all $(\boldsymbol{\pi}, \pi_0) \in \Pi$. We can show each case one by one.

- $d^*(\hat{\mathbf{y}}, \hat{\eta}) > 0$ iff there exists $(\hat{\boldsymbol{\pi}}, \hat{\pi}_0) \in \Pi$ such that $d(\hat{\mathbf{y}}, \hat{\eta} | \hat{\boldsymbol{\pi}}, \hat{\pi}_0) > 0$. This implies that $d^*(\hat{\mathbf{y}}, \hat{\eta}) > 0$ iff $(\hat{\mathbf{y}}, \hat{\eta}) \notin \mathcal{H}(\hat{\boldsymbol{\pi}}, \hat{\pi}_0)$ for some $(\hat{\boldsymbol{\pi}}, \hat{\pi}_0) \in \Pi$, thus $(\hat{\mathbf{y}}, \hat{\eta}) \notin \mathcal{E}$ (i.e., $(\hat{\mathbf{y}}, \hat{\eta})$ is in the exterior of \mathcal{E}).
- $d^*(\hat{\mathbf{y}}, \hat{\eta}) < 0$ iff $d(\hat{\mathbf{y}}, \hat{\eta} | \hat{\boldsymbol{\pi}}, \hat{\pi}_0) < 0$ for all $(\hat{\boldsymbol{\pi}}, \hat{\pi}_0) \in \Pi$. This implies that $d^*(\hat{\mathbf{y}}, \hat{\eta}) < 0$ iff $(\hat{\mathbf{y}}, \hat{\eta})$ is in the interior of $\mathcal{H}(\hat{\boldsymbol{\pi}}, \hat{\pi}_0)$ for all $(\hat{\boldsymbol{\pi}}, \hat{\pi}_0) \in \Pi$, thus $(\hat{\mathbf{y}}, \hat{\eta})$ is in the interior of \mathcal{E} .
- $d^*(\hat{\mathbf{y}}, \hat{\eta}) = 0$ iff $d(\hat{\mathbf{y}}, \hat{\eta} | \hat{\boldsymbol{\pi}}, \hat{\pi}_0) \leq 0$ for all $(\hat{\boldsymbol{\pi}}, \hat{\pi}_0) \in \Pi$, with at least one $(\hat{\boldsymbol{\pi}}, \hat{\pi}_0) \in \Pi$ such that $d(\hat{\mathbf{y}}, \hat{\eta} | \hat{\boldsymbol{\pi}}, \hat{\pi}_0) = 0$. This implies that $d^*(\hat{\mathbf{y}}, \hat{\eta}) = 0$ iff $(\hat{\mathbf{y}}, \hat{\eta}) \in \mathcal{H}(\hat{\boldsymbol{\pi}}, \hat{\pi}_0)$ for all $(\hat{\boldsymbol{\pi}}, \hat{\pi}_0) \in \Pi$ and there exists $(\hat{\boldsymbol{\pi}}, \hat{\pi}_0) \in \Pi$ such that $(\hat{\mathbf{y}}, \hat{\eta})$ is on the boundary of $\mathcal{H}(\hat{\boldsymbol{\pi}}, \hat{\pi}_0)$, thus $(\hat{\mathbf{y}}, \hat{\eta})$ is on the boundary of \mathcal{E} .

□

Theorem 2. *Epigraph distance functions are monotonic.*

Proof. Let $\alpha_i \in [0, 1]$ for $i = 1, 2$ and assume that $\alpha_2 > \alpha_1$. Define $(\bar{\mathbf{y}}^{(i)}, \bar{\eta}^{(i)}) = (1 - \alpha_i)(\mathbf{y}^0, \eta^0) + \alpha_i(\hat{\mathbf{y}}, \hat{\eta})$ for $i = 1, 2$. Since $0 \leq \alpha_1 < \alpha_2 \leq 1$, we may state $(\bar{\mathbf{y}}^{(1)}, \bar{\eta}^{(1)})$ as a convex combination of $(\bar{\mathbf{y}}^{(2)}, \bar{\eta}^{(2)})$ and (\mathbf{y}^0, η^0) of the following form

$$(\bar{\mathbf{y}}^{(1)}, \bar{\eta}^{(1)}) = \left(1 - \frac{\alpha_1}{\alpha_2}\right)(\mathbf{y}^0, \eta^0) + \frac{\alpha_1}{\alpha_2}(\bar{\mathbf{y}}^{(2)}, \bar{\eta}^{(2)}).$$

Convexity of d^* implies that

$$\begin{aligned} d^*(\alpha_1) &= d^*(\bar{\mathbf{y}}^{(1)}, \bar{\eta}^{(1)}) \leq \left(1 - \frac{\alpha_1}{\alpha_2}\right)d^*(\mathbf{y}^0, \eta^0) + \frac{\alpha_1}{\alpha_2}d^*(\bar{\mathbf{y}}^{(2)}, \bar{\eta}^{(2)}) = \frac{\alpha_1}{\alpha_2}d^*(\bar{\mathbf{y}}^{(2)}, \bar{\eta}^{(2)}) \\ &\leq d^*(\bar{\mathbf{y}}^{(2)}, \bar{\eta}^{(2)}) = d^*(\alpha_2), \end{aligned}$$

where the we have used $d^*(\mathbf{y}^0, \eta^0) = 0$ because $(\mathbf{y}^0, \eta^0) \in \partial\mathcal{E}$. Hence d is monotonic. □

Proposition 8. *Epigraph distance function $d_{\ell_p}^*$ (18) is strongly monotonic for any $p \geq 1$.*

Proof. The proof is exactly the same as Theorem 2, except

$$\begin{aligned} d_{\ell_p}^*(\alpha_1) &= d_{\ell_p}^*(\bar{\mathbf{y}}^{(1)}, \bar{\eta}^{(1)}) \leq \left(1 - \frac{\alpha_1}{\alpha_2}\right)d_{\ell_p}^*(\mathbf{y}^0, \eta^0) + \frac{\alpha_1}{\alpha_2}d_{\ell_p}^*(\bar{\mathbf{y}}^{(2)}, \bar{\eta}^{(2)}) = \frac{\alpha_1}{\alpha_2}d_{\ell_p}^*(\bar{\mathbf{y}}^{(2)}, \bar{\eta}^{(2)}) \\ &< d_{\ell_p}^*(\bar{\mathbf{y}}^{(2)}, \bar{\eta}^{(2)}) = d_{\ell_p}^*(\alpha_2), \end{aligned}$$

where the last strict inequality holds because $\frac{\alpha_1}{\alpha_2} < 1$ and $0 < d_{\ell_p}^*(\bar{\mathbf{y}}^{(2)}, \bar{\eta}^{(2)}) < \infty$ since $(\bar{\mathbf{y}}^{(2)}, \bar{\eta}^{(2)}) \notin \mathcal{E}$ and $d_{\ell_p}^*(\bar{\mathbf{y}}^{(2)}, \bar{\eta}^{(2)})$ measures the ℓ_q distance of $(\bar{\mathbf{y}}^{(2)}, \bar{\eta}^{(2)})$ to \mathcal{E} and is thus finite. □

Proposition 9. *Let $d_g(\hat{\mathbf{y}}, \hat{\eta} | \boldsymbol{\pi}, \pi_0) = \frac{\boldsymbol{\pi}^\top(\mathbf{b} - B\hat{\mathbf{y}}) + \pi_0(\mathbf{f}^\top\hat{\mathbf{y}} - \hat{\eta})}{g(\boldsymbol{\pi}, \pi_0)}$ be a normalized distance function. Then, the separation problem (21) is equivalent to the normalized separation problem (22). That is*

$$d_g^*(\hat{\mathbf{y}}, \hat{\eta}) = \max_{(\boldsymbol{\pi}, \pi_0) \in \Pi_g} \boldsymbol{\pi}^\top(\mathbf{b} - B\hat{\mathbf{y}}) + \pi_0(\mathbf{f}^\top\hat{\mathbf{y}} - \hat{\eta}).$$

Additionally, $g(\boldsymbol{\pi}, \pi_0) \leq 1$ is binding at optimality.

Proof. The separation problem (21) can be equivalently expressed as

$$\max_{q > 0} \left\{ \max_{(\boldsymbol{\pi}, \pi_0) \in \Pi; g(\boldsymbol{\pi}, \pi_0) = q} \frac{\boldsymbol{\pi}^\top(\mathbf{b} - B\hat{\mathbf{y}}) + \pi_0(\mathbf{f}^\top\hat{\mathbf{y}} - \hat{\eta})}{q} \right\}. \quad (55)$$

Define $(\tilde{\boldsymbol{\pi}}, \tilde{\pi}_0) = \frac{1}{q}(\boldsymbol{\pi}, \pi_0)$. Since Π is a cone it follows that $(\tilde{\boldsymbol{\pi}}, \tilde{\pi}_0) \in \Pi$. Additionally, since g is homogeneous, we have $g(\tilde{\boldsymbol{\pi}}, \tilde{\pi}_0) = \frac{1}{q}g(\boldsymbol{\pi}, \pi_0) = 1$. Therefore, the inner maximization in (55) can be restated as

$$\max_{(\tilde{\boldsymbol{\pi}}, \tilde{\pi}_0) \in \Pi; g(\tilde{\boldsymbol{\pi}}, \tilde{\pi}_0) = 1} \tilde{\boldsymbol{\pi}}^\top(\mathbf{b} - B\hat{\mathbf{y}}) + \tilde{\pi}_0(\mathbf{f}^\top\hat{\mathbf{y}} - \hat{\eta}), \quad (56)$$

which is constant with respect to q . Therefore, (55) itself is equivalent to (56). We next show that (56) is equivalent to (22), that is $g(\boldsymbol{\pi}, \pi_0) = 1$ can be replaced with $g(\boldsymbol{\pi}, \pi_0) \leq 1$. Let $(\hat{\boldsymbol{\pi}}, \hat{\pi}_0) \in \Pi_g$ be an arbitrary solution to (22) with $\hat{\alpha} = g(\hat{\boldsymbol{\pi}}, \hat{\pi}_0) < 1$. Note that $(\bar{\boldsymbol{\pi}}, \bar{\pi}_0) = \frac{1}{\hat{\alpha}}(\hat{\boldsymbol{\pi}}, \hat{\pi}_0) \in \Pi_g$ with $g(\bar{\boldsymbol{\pi}}, \bar{\pi}_0) = 1$. Additionally, we have

$$\bar{\boldsymbol{\pi}}^\top (\mathbf{b} - B\hat{\mathbf{y}}) + \bar{\pi}_0(\mathbf{f}^\top \hat{\mathbf{y}} - \hat{\eta}) = \frac{\hat{\boldsymbol{\pi}}^\top (\mathbf{b} - B\hat{\mathbf{y}}) + \hat{\pi}_0(\mathbf{f}^\top \hat{\mathbf{y}} - \hat{\eta})}{\hat{\alpha}} \geq \hat{\boldsymbol{\pi}}^\top (\mathbf{b} - B\hat{\mathbf{y}}) + \hat{\pi}_0(\mathbf{f}^\top \hat{\mathbf{y}} - \hat{\eta}),$$

which is strict if $\hat{\boldsymbol{\pi}}^\top (\mathbf{b} - B\hat{\mathbf{y}}) + \hat{\pi}_0(\mathbf{f}^\top \hat{\mathbf{y}} - \hat{\eta}) > 0$. Thus, at optimality $g(\boldsymbol{\pi}, \pi_0) \leq 1$ is binding. \square

Proposition 10. *Normalized distance function d_g induces a monotonic epigraph distance function d_g^* for any normalization function g .*

Proof. Since g is positive homogeneous, using Proposition 9, for any $(\bar{\mathbf{y}}, \bar{\eta})$ we may state $d^*(\bar{\mathbf{y}}, \bar{\eta})$ as

$$d_g^*(\bar{\mathbf{y}}, \bar{\eta}) = \max_{(\boldsymbol{\pi}, \pi_0) \in \Pi_g} \boldsymbol{\pi}^\top (\mathbf{b} - B\bar{\mathbf{y}}) + \pi_0(\mathbf{f}^\top \bar{\mathbf{y}} - \bar{\eta}),$$

where $\Pi_g = \{(\boldsymbol{\pi}, \pi_0) \in \Pi : g(\boldsymbol{\pi}, \pi_0) \leq 1\}$. This implies that d_g^* is convex, since it is the maximum of a number of linear functions. Therefore, by Theorem 2, d_g is monotonic. \square

Theorem 3. *Let d_g be a Benders normalized distance function with g a convex piece-wise linear function. Then BD Algorithm 2 converges to an optimal solution or asserts infeasibility of MP in a finite number of iterations.*

Proof. First, we show that the BD algorithm does not stagnate in a degenerate loop. Let $\hat{\Pi}_t$ be the set of dual solutions obtained before iteration t of the BD algorithm. Let $\text{MP}^{(t)}$ be the current approximation of MP with $(\mathbf{y}^{(t)}, \eta^{(t)})$ its optimal solution and let $(\bar{\boldsymbol{\pi}}, \bar{\pi}_0)$ be the dual solution obtained from BSP (21) for separating $(\mathbf{y}^{(t)}, \eta^{(t)})$. If $\bar{\boldsymbol{\pi}}^\top (\mathbf{b} - B\mathbf{y}^{(t)}) + \bar{\pi}_0(\mathbf{f}^\top \mathbf{y}^{(t)} - \eta^{(t)}) = 0$, then $(\mathbf{y}^{(t)}, \eta^{(t)})$ is optimal for MP since $\eta^{(t)}$ is a lower bound on the optimal value of MP. Hence, assume that $\bar{\boldsymbol{\pi}}^\top (\mathbf{b} - B\mathbf{y}^{(t)}) + \bar{\pi}_0(\mathbf{f}^\top \mathbf{y}^{(t)} - \eta^{(t)}) > 0$. Since $(\mathbf{y}^{(t)}, \eta^{(t)})$ is feasible for $\text{MP}^{(t)}$, it follows that $\hat{\boldsymbol{\pi}}^\top (\mathbf{b} - B\mathbf{y}^{(t)}) + \hat{\pi}_0(\mathbf{f}^\top \mathbf{y}^{(t)} - \eta^{(t)}) \leq 0$ for each $(\hat{\boldsymbol{\pi}}, \hat{\pi}_0) \in \hat{\Pi}_t$; hence, $(\bar{\boldsymbol{\pi}}, \bar{\pi}_0)$ cannot be a conical (i.e., scaling or a convex) combination of the solutions contained in $\hat{\Pi}_t$, meaning that, at each iteration, the BSP will produce a cut that is not implied by the cuts hitherto obtained.

Finally, since g is positive homogeneous and Π is a cone, by Proposition 9 we can restate the separation subproblem (21) as

$$\max_{(\boldsymbol{\pi}, \pi_0) \in \Pi_g} \boldsymbol{\pi}^\top (\mathbf{b} - B\mathbf{y}^{(t)}) + \pi_0(\mathbf{f}^\top \mathbf{y}^{(t)} - \eta^{(t)}), \quad (57)$$

where $\Pi_g = \{(\boldsymbol{\pi}, \pi_0) \in \Pi : g(\boldsymbol{\pi}, \pi_0) \leq 1\}$. Since g is a convex piece-wise linear function, Π_g is a polyhedron. Let Π_g^v and Π_g^r be the set of extreme points and rays of Π_g , respectively. Note that $\Pi_g^v \subset \Pi$ and $\Pi_g^r \subset \Pi$, and that they do not depend on $(\mathbf{y}^{(t)}, \eta^{(t)})$. If (57) is bounded, then its optimal solution is attained at one of the points in Π_g^v , otherwise an extreme ray belonging to Π_g^r causes unsoundness. Either way, the produced extreme point/ray of Π_g serves as the certificate. Therefore, the number of iterations is bounded by $|\Pi_g^v| + |\Pi_g^r|$. \square

Proposition 11. *The following relationship between the epigraph distance functions induced by d_{CB} , $d_{\ell p}$, and d_{RL1} holds:*

$$d_{\text{CB}}^*(\hat{\mathbf{y}}, \hat{\eta}) = Q(\hat{\mathbf{y}}) - \hat{\eta} \geq d_{\ell\infty}^*(\hat{\mathbf{y}}, \hat{\eta}) \geq \cdots \geq d_{\ell p}^*(\hat{\mathbf{y}}, \hat{\eta}) \geq \cdots \geq d_{\ell 1}^*(\hat{\mathbf{y}}, \hat{\eta}) \geq d_{\text{RL1}}^*(\hat{\mathbf{y}}, \hat{\eta}).$$

Proof. Recall that the $d_{\ell p}$, d_{RL1} , and d_{CB} distance functions are defined as

$$\begin{aligned} d_{\ell p}(\hat{\mathbf{y}}, \hat{\eta} | \boldsymbol{\pi}, \pi_0) &= \frac{\boldsymbol{\pi}^\top (\mathbf{b} - B\hat{\mathbf{y}}) + \pi_0 (\mathbf{f}^\top \hat{\mathbf{y}} - \hat{\eta})}{\|(\pi_0 \mathbf{f}^\top - \boldsymbol{\pi}^\top B, \pi_0)\|_p} \\ d_{\text{RL1}}(\hat{\mathbf{y}}, \hat{\eta} | \boldsymbol{\pi}, \pi_0) &= \frac{\boldsymbol{\pi}^\top (\mathbf{b} - B\hat{\mathbf{y}}) + \pi_0 (\mathbf{f}^\top \hat{\mathbf{y}} - \hat{\eta})}{\sum_{i=1}^m \pi_i \sum_{j=1}^n |B_{ij}| + (1 + \sum_{j=1}^n |f_j|) \pi_0} \\ d_{\text{CB}}(\hat{\mathbf{y}}, \hat{\eta} | \boldsymbol{\pi}, \pi_0) &= \frac{\boldsymbol{\pi}^\top (\mathbf{b} - B\hat{\mathbf{y}}) + \pi_0 (\mathbf{f}^\top \hat{\mathbf{y}} - \hat{\eta})}{\pi_0} \end{aligned}$$

The proof follows by noting the following facts:

(i) $\|\cdot\|_p \leq \|\cdot\|_{p'}$ for any $1 \leq p' < p$. This implies that

$$d_{\ell\infty}(\hat{\mathbf{y}}, \hat{\eta} | \boldsymbol{\pi}, \pi_0) \geq \cdots \geq d_{\ell p}(\hat{\mathbf{y}}, \hat{\eta} | \boldsymbol{\pi}, \pi_0) \geq \cdots \geq d_{\ell 1}(\hat{\mathbf{y}}, \hat{\eta} | \boldsymbol{\pi}, \pi_0) \quad \forall (\boldsymbol{\pi}, \pi_0) \in \Pi.$$

(ii) $\|(\pi_0 \mathbf{f}^\top - \boldsymbol{\pi}^\top B, \pi_0)\|_p \geq \pi_0$ for any $p \geq 1$. This implies that

$$d_{\text{CB}}(\hat{\mathbf{y}}, \hat{\eta} | \boldsymbol{\pi}, \pi_0) \geq d_{\ell\infty}(\hat{\mathbf{y}}, \hat{\eta} | \boldsymbol{\pi}, \pi_0) \quad \forall (\boldsymbol{\pi}, \pi_0) \in \Pi.$$

(iii) $\|(\pi_0 \mathbf{f}^\top - \boldsymbol{\pi}^\top B, \pi_0)\|_1 \leq \sum_{i=1}^m \pi_i \sum_{j=1}^n |B_{ij}| + (1 + \sum_{j=1}^n |f_j|) \pi_0$. This implies that

$$d_{\ell 1}(\hat{\mathbf{y}}, \hat{\eta} | \boldsymbol{\pi}, \pi_0) \geq d_{\text{RL1}}(\hat{\mathbf{y}}, \hat{\eta} | \boldsymbol{\pi}, \pi_0) \quad \forall (\boldsymbol{\pi}, \pi_0) \in \Pi.$$

Since the relationships follow for any $(\boldsymbol{\pi}, \pi_0) \in \Pi$, they must hold when each distance function is at maximum. \square